NOTE TO USERS

Université d'Ottawa · University of Ottawa

Université d'Ottawa · University of Ottawa

FACULTÉ DES ÉTUDES SUPÉRIEURES ET POSTDOCTORALES

FACULTY OF GRADUATE AND POSTDOCTORAL STUDIES

Lise MURPHY

AUTEUR DE LA THÈSE - AUTHOR OF THESIS

M. Sc.(Microbiology)

GRADE - DEGREE

Department of Biochemistry, Microbiology and Immunology

FACULTÉ, ÉCOLE, DÉPARTEMENT - FACULTY, SCHOOL, DEPARTMENT

TITRE DE LA THÈSE - TITLE OF THE THESIS

Regulation of human parainfluenza virus type 3 fusion protein expression

K. Dimock

DIRECTEUR DE LA THÈSE - THESIS SUPERVISOR

CO-DIRECTEUR DE LA THÈSE - THESIS CO-SUPERVISOR

EXAMINATEURS DE LA THÈSE - THESIS EXAMINERS

E. Brown

M. Holcik

J.-M. De Koninck, Ph.D

LE DOYEN DE LA FACULTÉ DES ÉTUDES SUPÉRIEURES ET POSTDOCTORALES

DEAN OF THE FACULTY OF GRADUATE AND POSTDOCTORAL STUDIES

REGULATION OF HUMAN PARAINFLUENZA VIRUS TYPE 3 FUSION PROTEIN EXPRESSION

A Thesis Submitted to the

School of Graduate Studies

University of Ottawa

In Partial Fulfillment of the Requirements for the Degree of

Master of Science

Department of Biochemistry, Microbiology and Immunology

Faculty of Medicine

By

Lise Murphy

Your file Votre référence
ISBN: 0-494-01558-6
Our file Notre référence
ISBN: 0-494-01558-6

ABSTRACT

Human parainfluenza virus type 3 (HPIV3) is an enveloped, negative-strand, non-segmented RNA virus. HPIV3 is a human respiratory pathogen that primarily causes diseases such as croup, bronchiolitis and pneumonia in children. The virus has two glycoproteins that allow it to interact with host cells, the receptor binding protein hemagglutinin-neuraminidase (HN) and the fusion protein (F), which enables the virus to enter the cell by fusion of the viral envelope to the target cell plasma membrane.

This research was initiated with the goal of determining mechanisms by which HPIV3 regulates the expression of the fusion protein. Evidence indicated that the transcription of the F gene differed from that of the other genes because there was a very high level of read-through transcription at the junction of the matrix (M) gene and the F gene. This read-through transcription caused >80% of the potential F gene transcripts to be present in biscistronic M/F mRNA, in which the F open reading frame cannot be translated. I hypothesized that the read-through transcription is a means of regulating the amount of F protein synthesized in the infected cell, and that the virus may also have evolved post-transcriptional mechanisms to regulate F protein expression. The F gene also has a 5' untranslated region (5' UTR) that is much longer than the 5'UTRs of the five other HPIV3 genes, which may affect the efficiency of translation of the F protein. In addition, the F protein must be cleaved in the Golgi apparatus in order to become functional, however, the F protein precursor is only partially cleaved in infected cells. This is another potential method to control the amount of functional (ie. fusion active) F protein. Therefore, this study

focussed on the regulation of F expression by post-transcriptional mechanisms including the possible roles played by a long 5' UTR and the inefficient cleavage of the F precursor by the cellular protease, furin.

The first objective was to assess the potential effects of the long 5' UTR of the F mRNA on translation. Plasmids were constructed in which the 5' UTR of each of the HPIV3 mRNAs was placed immediately upstream of the chloramphenicol acetyl transferase (CAT) coding sequence. The effect of the 5' UTRs on CAT synthesis were evaluated following *in vitro* transcription and *in vitro* translation of the mRNAs. Contrary to the original prediction that the long 5' UTR of the F mRNA would decrease CAT expression, expression of CAT from mRNAs containing the NP, P, M and F 5' UTRs was similar. Interestingly, expression of CAT was reduced when the CAT coding sequence was preceded by the C, HN or L 5' UTR, suggesting that the sequences of these 5' UTRs decrease translation efficiency.

The next objective was to determine if more efficient cleavage of the F precursor would have effects on membrane fusion. I constructed a plasmid encoding an F protein that I predicted would be cleaved by furin more efficiently than the parental protein. When the fusion properties of the two proteins were compared, following transfection of cells with the two plasmids, the mutant F protein consistently exhibited a higher fusion index than the unmodified F protein. Western blot analysis of the F proteins in cell lysates showed little or no difference in the level of expression or the extent of cleavage in the absence of the HN protein. However, in the presence of the HN protein, the mutant F protein was cleaved

approximately 1.4 times more efficiently than the parental F protein, which may account for the observed differences in fusogenicity.

ACKNOWLEDGMENTS

I would like to thank Ken, for his perseverance and encouragement. Thank you for always believing in me and the project when I had doubts. You are by far one of the best supervisors out there and anyone lucky enough to have had you knows it! I would like to acknowledge all the laboratory expertise that was passed on to me by Neil and Reza (I've developed a number of their bad habits, as well as a few of my own!!). I would also like to thank David for his ear, he was never too busy to listen. Labmates past and present who helped, encouraged and entertained.

I would also like to thank my parents and my in-laws for their faith, encouragement and proof-reading (thank you Sheila). Last but by far not least, I want to thank Bradley for his love, patience and sense of humour.

TABLE OF CONTENTS

LIST OF FIGURES

LIST OF TABLES

LIST OF ABBREVIATIONS

ABTS	2-2'-azino-bis[3-ethylbenz-thiazoline-6-sulfonic acid]
ATCC	American Type Culture Collection
β-Gal	beta galactosidase
bp	base pairs
BSA	bovine serum albumin
CAT	chloramphenicol acetyltransferase
cDNA	complementary DNA
CPRG	chlorophenol red-β-D-galactopyranoside
CV-1	African green monkey kidney cell line
DEPC	diethyl pyrocarbonate
EDTA	ethylene diamine tetraacetic acid
EtBr	ethidium bromide
F	fusion protein
FBS	fetal bovine serum
GE	gene end sequence
GS	gene start sequence
HEp-2	human epidermal carcinoma cell line
HPIV3	human parainfluenza virus type 3
HN	hemagglutinin-neuraminidase protein
IG	intergenic sequence

L	large polymerase submit
LB	Luria-Bertani
LLC-MK2	rhesus monkey kidney cell line
Luc	luciferase
M	matrix protein
MOI	multiplicity of infection
mRNA	messenger ribonucleic acid
MV	measles virus
NDV	Newcastle disease virus
NP	nucleoprotein
nt	nucleotide
ORF	open reading frame
P	polymerase associated phosphoprotein
PCR	polymerase chain reaction
pfu	plaque forming units
RNP	ribonucleoprotein
RSV	respiratory syncytial virus
RT	read-through transcription
SDS	sodium dodecyl sulphate
SeV	sendai virus
SV5	simian virus 5
TAE	tris/acetate/EDTA buffer

TBE	tris/borate/EDTA buffer
TBS	tris buffered saline
TOP	terminal oligopyrimidine tract
uAUG	upstream start codon
uORF	upstream open reading frame
UTR	non-translated region
vTF7-3	recombinant vaccinia virus encoding T7 RNA polymerase
VWR	Western Reserve vaccinia virus strain

I. INTRODUCTION

A. *Paramyxoviridae*

Negative-strand RNA viruses are enveloped viruses that infect many different hosts (Conzelmann, 1998). Members of this group of viruses, which encompasses many families, include important human pathogens such as influenza virus, measles virus, mumps virus, Ebola virus and economically important animal viruses such as Newcastle disease virus (NDV), rinderpest virus (RPV) and rabies virus (Neuman *et. al.*, 2002). One of the four families that make up the order *Mononegavirales*, the non-segmented branch of the negative-strand RNA viruses, is the family *Paramyxoviridae* (Conzelmann, 1998). This family is comprised of negative-strand RNA viruses that contain a host cell plasma membrane-derived lipid bilayer envelope (Lamb and Kolakofsky, 2001). The morphology of the *Paramyxoviridae* is generally spherical but can be pleiomorphic (Lamb and Kolakofsky, 2001). The family *Paramyxoviridae* is composed of two subfamilies, *Paramyxovirinae*, which contains three genera: 1) Respirovirus, which includes human parainfluenza viruses types 1 and 3 (HPIV1/3), 2) Rubulavirus, which includes human parainfluenza viruses types 2 and 4 (HPIV2/4), mumps virus and Newcastle disease virus (NDV), and 3) Morbillivirus which includes measles virus (Lamb and Kolakofsky, 2001). The subfamily *Pneumovirinae* contains the genus Pneumovirus which includes human respiratory syncytial virus (hRSV) and metapneumovirus (Lamb and Kolakofsky, 2001).

The virus of interest in this thesis is human parainfluenza virus type 3 (HPIV3).

Figure 1 is a schematic of the HPIV3 virion. There are four human parainfluenza viruses that primarily affect children and infants (Chanock *et al.*, 2001; Henrickson, 2003). HPIV1 and HPIV2 cause mainly croup and HPIV3 is an important cause of croup, pneumonia and bronchiolitis (Chanock *et al.*, 2001). The data regarding HPIV4 are incomplete, however, it does appear to cause all the respiratory tract syndromes (Henrickson, 2003). In the United States, children under five are affected by more than five million lower respiratory infections annually. HPIV1, HPIV2 and HPIV3 are responsible for one-third of these infections and, together, are only second to RSV as a cause of hospitalization for viral lower respiratory tract infections (Henrickson, 2003). Unfortunately, although most children have antibodies to the HPIVs, immunity is incomplete and susceptibility to infection is lifelong (Henrickson, 2003). Infants younger than 6 months of age are particularly susceptible to HPIV3 infection, and this virus hospitalizes 18 000 infants and children annually (Henrickson, 2003). In the developed world, mortality due to HPIV infection is rare, generally limited to infants, the elderly and the immunocompromised (Henrickson, 2003). However, in developing countries, preschool-aged children are at risk of HPIV-induced death from either the primary infection or bacterial complications (Henrickson, 2003).

1. Genome

The HPIV3 genome, in fact the genome of all the Respiroviruses, contains six

Figure 1 **Schematic of the HPIV3 virion.** The components are as follows: nucleocapsid protein, NP; polymerase-associated phosphoprotein, P; matrix protein, M; fusion glycoprotein, F; hemagglutinin-neuraminidase glycoprotein, HN; large polymerase subunit, L. The odd shape is to denote a pleiomorphic structure. NP, P and L are associated with the negative sense RNA genome and form the ribonucleoprotein, RNP. This schematic is not drawn to scale.

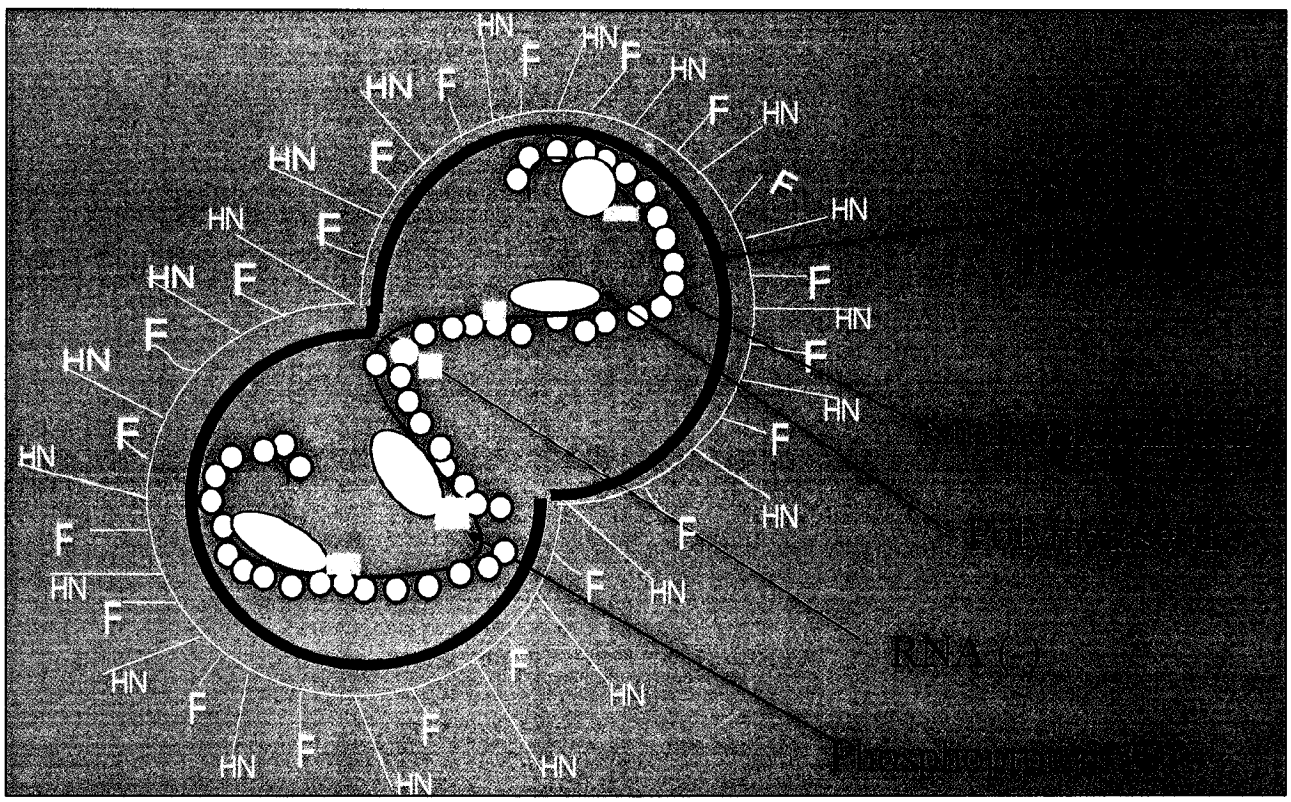
HN
F
RNA (-)

genes, and begins with a 3' leader sequence and ends with a 5' trailer sequence. The order of the genes is shown in Figure 2. The length of the HPIV3 genome is 15 462 nucleotides (nts) (Chanock *et al.*, 2001). The first gene encodes the nucleocapsid protein (NP) which is essential for encapsidation of the genome, and formation of the nucleocapsid or ribonucleoprotein (RNP) (Lamb and Kolakofsky, 2001). Interestingly, NP does not have any known RNA-binding domains and does not interact with RNA on a Northwestern blot, when it is transferred to nitrocellulose (Lamb and Kolakofsky, 2001). NP is one of the most abundant proteins in the virion, having approximately 2600 copies (Chanock *et al.*, 2001). The next gene in the HPIV3 genome encodes the phosphoprotein (P), as well as the C, D and V proteins (Lamb and Kolakofsky, 2001). P is a cofactor of the polymerase, L (Lamb and Kolakofsky, 2001). The carboxyl-terminus of the P protein contains domains required for binding to the NP protein to form the RNP as well as the domain that binds with the L protein to form the active polymerase (Lamb and Kolakofsky, 2001). The C protein is a basic, non-structural protein that associates with the RNP, and binds L. Translation of the C protein begins in an alternative reading frame just downstream of the P protein initiation codon, and the C protein has been shown to inhibit both transcription and replication. Its ablation strongly attenuates HPIV3 replication *in vitro* and *in vivo* (Chanock *et al.*, 2001). The D protein, whose function is unknown, is the result of the non-templated addition of two Gs resulting in a frameshifted protein (Chanock *et al.*, 2001). There is a putative V open reading frame (ORF), which would be the result of non-templated addition of one G at the RNA editing site, however, the mechanism for accessing this ORF is unknown due to stop codons between the editing site and the ORF (Chanock *et al.*, 2001). The third gene in the

Figure 2 **HPIV3 genome organization** (3' to 5', negative sense RNA). Genes are shown in the order in which they appear in the genome, each gene is drawn to scale as a proportion of the total 15 462 nucleotides. The gene end sequences, GE are in blue, the intergenic sequences, IG are in green and the gene start sequences, GS are in purple. The junction sequences for NP/P and P/M are identical as are F/HN and HN/L. The 8 additional nucleotides in the M gene end sequence are underlined in red.

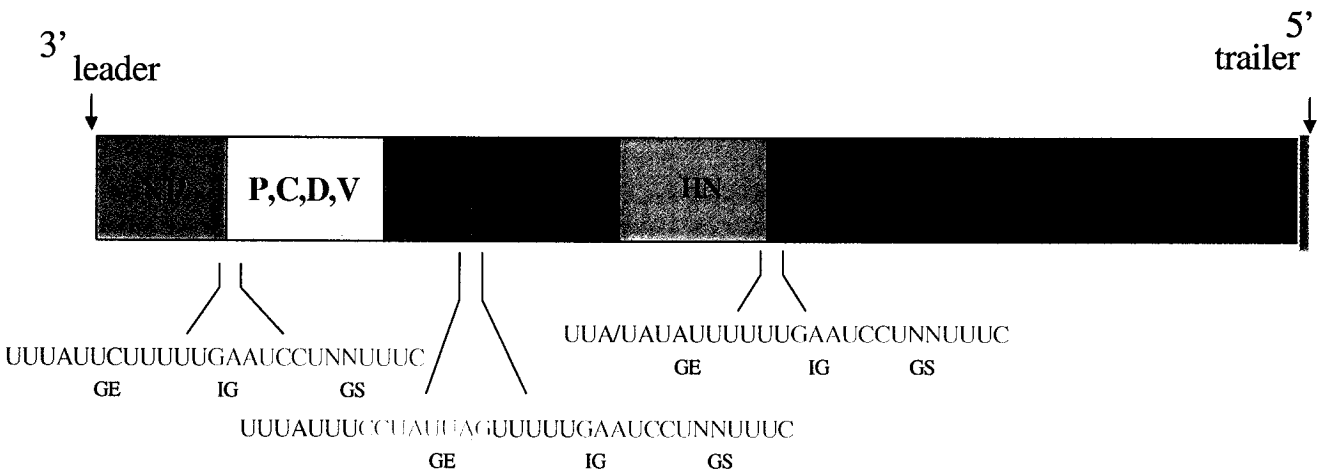
3'
leader
5'
trailer
P,C,D,V
HN
UUUAUUCUUUUUGAAUCCUNNUUUC
GE
IG
GS
UUA/UAUAUUUUUUGAAUCCUNNUUUC
GE
IG
GS
UUUAUUUCCUAUUAGUUUUUGAAUCCUNNUUUC
GE
IG
GS

HPIV3 genome encodes the matrix protein (M). The matrix protein underlies the lipid bilayer and interacts with the cytoplasmic tails of the two envelope glycoproteins (Lamb and Kolakofsky, 2001). The matrix protein is known as the "central organizer of viral morphogenesis" (Lamb and Kolakofsky, 2001) and is believed to play a pivotal role in viral budding because of its self-association as well as its interactions with the nucleocapsid, the envelope and the cytoplasmic tail of the two integral membrane proteins (Lamb and Kolakofsky, 2001). M is the most abundant protein in the virion with approximately 3000 copies per virion (Chanock *et al.*, 2001).

The fourth gene in the HPIV3 genome encodes the fusion protein (F), a glycosylated type I integral membrane protein that spans the membrane once and is responsible for mediating the fusion of the viral envelope with the host cell plasma membrane (Lamb and Kolakofsky, 2001). The fifth gene encodes the attachment protein, the hemagglutinin-neuraminidase protein (HN) (Lamb and Kolakofsky, 2001). HN is a type II integral protein that spans the membrane once and is responsible for attachment of the virus to the receptor, sialic acid, on the surface of the target cell membrane (Lamb and Kolakofsky, 2001). This protein can cause agglutination of red blood cells and also has a neuraminidase function, which cleaves sialic acid, and may aid in virus release from infected cells (Lamb and Kolakofsky, 2001).

The sixth and final gene of the HPIV3 genome encodes the viral RNA dependent RNA polymerase (L). There are approximately 50 copies of this protein per virion, making

it the least abundant structural protein (Lamb and Kolakofsky, 2001).

2. Overview of Virus Transcription and Replication

The genome of the negative-strand RNA viruses can be segmented or non-segmented (order *Mononegavirales*). However, the general method of replication and transcription is universal to all negative-strand RNA viruses (Conzelmann, 1998). The genome is found in a ribonucleoprotein complex, RNP, which is a tight, helical protein structure surrounding the RNA (Conzelmann, 1998). The RNA is never dissociated from the RNP, which is, essentially, the mandatory template for replication and transcription (Conzelmann, 1998). The RNP of negative-sense, nonsegmented RNA viruses consists of a complex of proteins including the nucleoprotein, NP, the phosphoprotein, P and the RNA dependent RNA polymerase, L (Conzelmann, 1998). In the cytoplasm of the infected cell, before the accumulation of viral proteins, the viral polymerase only transcribes the leader RNA and the mRNAs, beginning from the 3' end of the genome, reinitiating mRNA transcription after encountering transcriptional regulatory sequences at the junctions between each gene (gene end and gene start sequences)(Lamb and Kolakofsky, 2001). The transcription of viral genes is considered to be initiated at a single site at the beginning of the leader sequence. The polymerase transcribes the leader mRNA and then re-initiates at the start of the NP gene. The polymerase complex transcribes the NP gene, then stutters at the short poly U tract near the end of the gene, allowing polyadenylation. The polymerase is then able to re-initiate transcription at the "gene start" motif of the P gene. This process continues for each gene.

A finite number of polymerase molecules fail to re-initiate transcription and dissociate from the genome at each gene junction, resulting in a gradient of transcription from the 3' end to the 5' end of the genome. (Conzelmann, 1998)

The process of viral replication begins once the viral proteins have started to accumulate, most importantly NP. In this process, the viral polymerase reads through the gene end signals, does not polyadenylate the mRNAs and generates a full length complementary copy, the antigenome, which is also found in a RNP complex (Lamb and Kolakofsky, 2001). Due to the complex nature of the negative-strand virus genome, molecularly engineered viruses from cloned cDNA were generated almost fifteen years after those of positive strand viruses and rescue of these viruses from DNA remains a tedious method (Neumann *et al.*, 2002).

The first step in the virus life cycle is fusion of the viral membrane to the host cell lipid bilayer (see below). Once fusion has occurred, the HPIV3 RNP is ejected into the cytoplasm of the cell (Henrickson, 2003). Transcription causes the viral proteins to accumulate which allows replication of the genome to occur. The genome is first synthesized as a positive RNA strand and from this strand, the appropriate negative strand RNA genome is encapsidated with NP protein. This RNP could be used for additional cycles of transcription and replication or it could be packaged as a new virion (Henrickson, 2003).

3. The Fusion protein and membrane fusion

The F protein of paramyxoviruses is synthesized as a precursor protein, F_0, that is cleaved in the trans Golgi into two disulfide linked subunits, F_1 and F_2 (Chanock *et al.*, 2001). This cleavage is carried out by a KEX-like protease whose recognition sequence is R-X-K/R-R (Chanock *et.al.*, 2001; Nakayama, K. 1997). The evidence suggests that this enzyme is furin (Ortmann *et. al.*, 1994). Figure 3A depicts the structure of the HPIV3 F protein. The fusion peptide is a 25 residue hydrophobic peptide located just after the cleavage site at the N-terminus of the F1 subunit (Lamb and Kolakofsky, 2001). Among *Paramyxovirinae*, the fusion peptides are highly conserved, with between 68-84% identity (Lamb and Kolakofsky, 2001). The fusion peptide begins the fusion process by inserting itself into the host cell membrane (Lamb and Kolakofsky, 2001). Mutagenesis studies of the fusion peptide demonstrated that when the glycine residues at positions 3, 7 or 12 were changed to alanine, there was a significant increase in syncytium formation. Syncytia are multinucleated cells that can result from virus induced cell to cell fusion (Maresova, *et al.*, 2001).

The widely accepted model for paramyxovirus fusion involves insertion of the fusion peptide into the target membrane (Joshi *et al.*, 1998). Then there is an interaction between the heptad repeats of the three fusion proteins in the trimer (Joshi *et al.*, 1998). A heptad

Figure 3 **Schematic representation of the HPIV3 F protein.** A) The fusion protein precursor, F_0, is cleaved by furin and F_1 and F_2 are joined by a disulfide bond. The fusion peptide, FP, is located at the N-terminus of the F_1 subunit and is a hydrophobic domain (dark green). The two heptad repeats, HRN and HRC, are separated by a segment that is approximately 250 amino acids long and is cysteine rich. The transmembrane, TM, domain is a hydrophobic domain (dark green). The C-terminus of the F_1 subunit is the cytoplasmic domain, CT. B) The heptad repeats of different viruses; murine Moloney leukemia virus Env-TM protein, HIV gp41, Ebola virus GP2, SV5 F protein and influenza virus HA. Reproduced with permission from publisher Lippincott Williams & Wilkins (Lamb and Kolakofsky, 2001).

A)

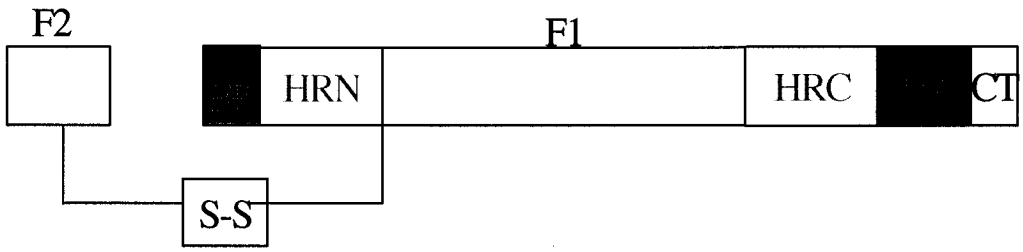

B)

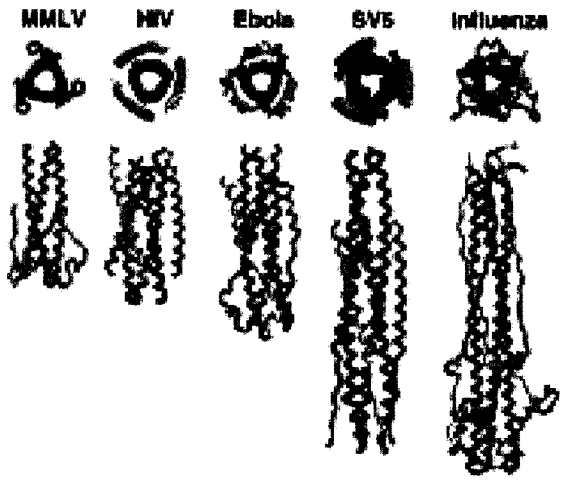

repeat is a tandem repeat sequence in a protein, in which the 3rd and the 7th amino acid is a hydrophobic residue, see Figure 3B (Young *et al.*, 1997). This allows the formation of a coiled-coil structure. The N-terminal heptad repeat interacts with the C-terminal heptad repeat, forming a trimer of dimers (the F protein is a homotrimer) (Joshi *et al.*, 1998). The N-terminal heptad repeats form the core of the hexameric complex and the C-terminal heptad repeats are on the exterior of this core (Joshi *et al.*, 1998). This complex pulls the two membranes close enough together to overcome the barriers to fusion and fusion occurs (Joshi *et al.*, 1998).

One thing missing from the description of the previous model was the role of HN in fusion. The HPIV3 F protein cannot cause fusion independently, there is evidence for an interaction between F and HN (Stone-Hulslander and Morrison, 1997; Tanaka *et al.*, 1996; Porotto *et al.*, 2003). There are two proposed models for this interaction. In the first, HN undergoes a conformational change upon binding to sialic acid that allows it to interact with F, rendering F fusion-active (Porotto *et al.*, 2003). The second model is that F and HN interact early in the Golgi network and upon HN binding to sialic acid, both proteins undergo conformational changes, HN releases F, resulting in the exposure of the the fusion peptide (Porotto *et al.*, 2003). Therefore, in order to reproduce fusion in cell culture, both F and HN cDNA must be transfected into cells.

There are a number of structural peculiarities of the F gene and mRNA. The first is that the M gene end motif contains 8 nucleotides more than the gene end motifs of the five

other genes. This affects the transcription of the F gene (discussed in greater depth below), by causing read-through transcription of the F gene. The F mRNA also has a 5' untranslated region (5'UTR) that is approximately 2.4 to 16 times longer than the 5'UTR of the other HPIV3 mRNAs.

B. Transcriptional Regulation

Since viruses are so small and carry as little genetic material as needed, they have evolved many very interesting ways of regulating the expression of their proteins. Some of these mechanisms are at the level of transcription of the genome to message. HPIV3, like many of the negative strand viruses utilizes the genome organization itself as a major mechanism for the regulation of gene product expression. There is only one transcriptional entry site in the genome, at the 3' end (Chanock *et al.*, 2001, Conzelmann, 1998). The first 13 nucleotides of the leader sequence are the putative transcriptional promoter (Chanock *et al.*, 2001, Lamb and Kolakofsky, 2001). The RNA dependent RNA polymerase scans the genome from the 3' end, recognizing transcriptional initiation and termination signals and polyadenylates each message by reiterating a short tract of Us in the gene end motif. The only sequence that is not transcribed is a highly conserved intergenic trinucleotide, GAA, as depicted in Figure 2 (Chanock *et al.*, 2001). Since transcription cannot initiate *de novo* internally on the genome, and because after each gene the polymerase stutters to polyadenylate each mRNA, there is a gradient in the quantity of transcripts formed, because some polymerase molecules dissociate from the genome during these processes

(Conzelmann, 1998). Therefore, the genes at the 3' end of the genome are transcribed in greater abundance (e.g. NP), and the amount of each mRNA decreases with increasing distance from the 3' terminus, so that genes at the 5' end of the genome are transcribed less frequently (e.g. L).

The amount of polymerase that fails to reinitiate transcription of the downstream gene has been quantified for Vesticular Stomatitis Virus (VSV) and is approximately one third (Conzelmann, 1998).

Another way that certain viruses regulate the amount of mRNA available for translation is by transcribing bicistronic mRNAs. Wong and Hirano (1987) determined that only the first cistron of a replica of the measles virus bicistronic P and M mRNA was translated. If the viral genome contained sequences that promote read-through transcription this would be an important mechanism for downregulating the amount of the second cistron available for translation. It has been demonstrated that HPIV1 has significant read-through transcription at the M-F gene junction, causing 80% of F mRNAs to be bicistronic, the other 20% are normal monocistronic mRNAs (Bousse *et. al.*, 1997). Simian virus 5 (SV5) also employs this tactic, approximately 40% of the SV5 F mRNA is bicistronic (Rassa and Parks, 1998). Interestingly, a study that attempted to determine what motifs were responsible for the HPIV1 read-through transcription pinpointed not only the M gene end signal and the start signal of F but also the long 5'UTR of HPIV1 F. They found that reducing the length of the F 5'-UTR from 264 nucleotides to 31 nucleotides decreased read-through from 23 to 6%

(Bousse *et. al.*, 2002).

All of the HPIV3 genes transcripts are present as bicistronic mRNA, although the percentage of read-through at each gene junction varies. There is no quantitative evidence for HPIV3 read-through in infected cells, there is evidence for M/F bicistronic mRNA in infected LLC-MK2, hybrid select translation proved that this mRNA only codes for M protein (Dimock *et al.*, 1987). In a minigenome system, the percentage read-through at the NP/P, F/HN and the HN/L gene junctions was 10%, 16% and 23% respectively, but 88% at the M/F junction (Jogalakar, 2000). The M and F genes of HPIV3, like those of HPIV1 also produce read-through transcription. The mechanism for this read-through, however, is different from what has been observed for M/F readthrough for HPIV1. The HPIV3 M gene end signal varies from that of the consensus sequence by the "insertion" of 8 extra nucleotides. Work in the Dimock lab using minigenomes has demonstrated that these 8 extra nucleotides are necessary and sufficient to cause read-through transcription (Jogalakar, 2000).

C. Translational Regulation

There are a number of ways that gene products can be regulated at the level of translation. The 5' untranslated region (5'UTR) of the mRNA is a key player for translational regulation. Depending on the length, secondary structure, the presence of upstream open reading frames (uORFs) or upstream start codons (uAUGs) the 5'UTR can extensively regulate the amount of a gene product that is expressed. An uORF is a ORF that is initiated

upstream of the desired gene product; generally uORFs are very short, (ie 4-20 codons). Davuluri *et. al.* (2000) have grouped genes in three classes following extensive computational analysis of the 5' UTR sequences. Class I mRNAs encode poorly translated proteins such as transcription factors and regulatory proteins. Class II mRNAs have a terminal oligopyrimidine tract (TOP) and are regulated in a growth dependent fashion (Davuluri *et. al.* 2000). A TOP is a stretch of 4-14 pyrimidines that always starts with a C at the cap site (Meyuhas, 2000). Finally, class III mRNAs are highly expressed genes that are transcriptionally regulated and most likely efficiently translated (Davuluri *et. al.* 2000). In fact Davuluri *et. al.* have determined the most discriminatory variables between the three classes of mRNAs that they have described. Some of these values are the presence of a TOP, the 5' UTR length, the presence of a stable secondary structure within the first 100 bases from the cap site, the A/T and G/C ratios, the number of uAUGs and the number of uORFs.

According to Kozak, in a eukaryotic system, the 40S ribosomal subunit loaded with the Met-tRNA$_i^{met}$ linearly scans the mRNA, beginning at the cap, and recognizes the first AUG through base-pairing (Kozak, 1997). This causes the 40S subunit to stop, allowing the recruitment of the 60S ribosomal subunit, thus forming the 80S ribosome which allows translation to occur (Kozak 1997). The sequence surrounding the AUG (the context of the AUG) can modify its ability to stop the 40S subunit (Kozak, 1997). The consensus sequence is GCCA/GCC$\underline{a^{+1}ug}$G, and the A at position -3 and the G at position +4 have the strongest effects, together modulating translation as much as 10 fold (Kozak, 1991, 2002). It has been shown that if the consensus sequence is adhered to perfectly, or if the AUG is surrounded by

ANNaugN or GNNaugG, almost all of the ribosomes initiate at that AUG (Kozak, 2002). It has also been demonstrated that when the context is weak, ie. lacking both the purine at position -3 as well as the G at position +4, some ribosomes initiate there, however, most continue scanning (Kozak, 2002). This is termed leaky scanning (Kozak, 2002).

Leaky scanning as well as reinitiation are employed by a number of viruses including reovirus and influenza virus (Dawe and Duncan, 2002; Chen *et al.*, 2001). Baboon reovirus is an interesting virus in that it is among the few members of the family *Reoviridae* that induce syncytium formation; which is striking because reoviruses are nonenveloped (Dawe and Duncan, 2002). A recently uncovered fusion-associated small transmembrane protein has been determined to be in a dicistron with another protein (Dawe and Duncan, 2002). The mechanism has not been fully elucidated, but the first cistron is located 388 nucleotides upstream of the second and its sequence overlaps with the second by 38 nucleotides (Dawe and Duncan, 2002). The first AUG is not in a preferred context: GUACaugG, but nonetheless encodes the fusion associated protein, p15 (Dawe and Duncan, 2002). The second cistron, which codes for the p16, protein starts at one of two consecutive AUGs, both of which have a purine at position -3 and +4 (Dawe and Duncan, 2002). Before the start codon of the second cistron, there are two other AUGs in weak translational context (Dawe and Duncan, 2002). The authors suggest that leaky scanning accounts for the translation of both cistrons (Dawe and Duncan, 2002).

Influenza A virus encodes a protein named PB1-F2 in the +1 reading frame of PB1,

which induces apoptosis in monocytic cells in culture (Chen *et al.*, 2001). The start codon for this protein is 94 nucleotides downstream of the start codon for the PB1 gene (Chen *et al.*, 2001). The start codon for PB1 is in a suboptimal context for initiation not having either an A or G at position -3, but having a G at position +4 (Chen *et al.*, 2001). The start codon for PB1-F2 is the third AUG after the start codon for PB1, the two other AUGs are also in suboptimal context, but the AUG for PB1-F2 is in a good context having both a G at position -3 and position +4 (Chen *et al.*, 2001). The authors predict that ribosomal leaky scanning is responsible for the initiation at the PB1-F2 AUG as a means of generating another product from a single gene (Chen *et al.*, 2001).

D. Proteolytic cleavage as a means of regulation

Many organisms, such as eukaryotic cells, plant cells, animal and plant viruses use protein cleavage as a means of regulating gene expression. Proteases, such as trypsinogen, chymotrypsinogen and pro-furin, themselves must be cleaved to become active (Leduc, *et al.*, 1992; Nakayama, 1997; Voet and Voet, 1998). Trypsin is the activator of many zymogens and proenzymes such as proelastase, chymotrypsinogen, procarboxypeptidase and prophospholipase A_2 (Sandberg and Borgström, 2002; Seidah and Chrétien, 1997; Voet and Voet, 1998). Prohormones are also proteolytically processed for activation. Prohormones such as proinsulin, proglucagon, prorenin, and proPTH (parathyroid hormone) are all cleaved by a group of proteases named the proprotein convertases (Seidah and Chrétien, 1997). There is a group of proprotein convertases called subtilisin/Kex2p-like proprotein

convertases, which includes Kex2 from yeast, furin, PC2, PACE4 and others (Nakayama, 1997). Furin, expressed ubiquitously in mammalian cells, is responsible for the processing of a broad assortment of precursor proteins (Nakayama, 1997; Seidah and Chrétien, 1997), for example, furin is responsible for the activation of many proteins, some of which are pro-TGFβ (tumour growth factor), pro-FactorIX and pro-FactorX, pro-PTH, and the insulin receptor, as well as various viral envelope glycoproteins (Nakayama, 1997; Seidah and Chrétien, 1997). Among these viral glycoproteins are HIV-gp160, RSV F protein, influenza hemagglutinin, NDV F protein, measles virus F protein and HPIV3 F protein (Nakayama, 1997; Seidah and Chrétien, 1997). Watanabe, *et al.* (1993) describes the following rules with regards to furin cleavage: i) an Arg at position -1 relative to the cleavage site is indispensable; ii) in addition to the Arg at position -1, at least two of the three positions: -2, -4 and -6 must have a basic amino acid for efficient cleavage (if all three residues are basic, the result is the most efficient cleavage); iii) a hydrophobic aliphatic amino acid at position +1 is not desirable (Watanabe *et al.*, 1993).

Previous experiments in Ken Dimock's lab have shown that in HPIV3 infected cells, on the surface of HPIV3 virions and in F transfected cells, the cleavage of F_0 to F_1 and F_2 is incomplete (Ebata, 1996 ; McKenna, unpublished results; Storey, 1987). D. Storey showed that cleavage of F was only 50% cleaved on the surface of HPIV3 virions (Storey, 1987). This phenomenon is not limited to HPIV3. Uncleaved measles virus F is also packaged into measles virions (Watanabe *et al.*, 1995). The cleavage sites in HPIV3 and measles virus are not optimal.

E. Overview

Human parainfluenza virus type 3 (HPIV3), is a negative sense RNA virus that infects the lower respiratory tract and can cause serious complications, especially in children of developing countries (Henrickson, 2003). The goal of this research was to better understand the regulation of expression of the HPIV3 fusion protein, F. F is one of two HPIV3 glycoproteins, and is an essential component in viral entry into host cells as well as target for humoral immune response against HPIV3 (Henrickson, 2003).

At first glimpse, the expression of F is not favoured; more than half of the F sequences transcribed into mRNA are present downstream of matrix (M) protein coding sequences in a bicistronic mRNA and cannot be translated into F protein. Another interesting feature of F mRNA is that its 5' UTR is 192 nts long, much longer than the 5' UTR of any of the other HPIV3 mRNAs, and this may negatively regulate F protein synthesis. Finally, F is translated as a precursor protein, F_0, that must be cleaved into F_1 and F_2 in order to be fusion active. Approximately half of HPIV3 F_0 present in infected cells is cleaved. Why does the virus appear to go to such great pains to reduce the amount of functional F protein expressed in infected cells? Is it possible that if excessive amounts of functional F protein are expressed in cells, there would be too much fusion, and the resulting cell death would be detrimental to virus replication? In fact, Lamb and Kolakofsky put forward that there may be a "balance between high fusion activity and successful viral

replication, as high fusion activity is deleterious to cell viability" (Lamb and Kolakofsky, 2001). Another possibility is that "overexpression" of the F protein would lead to downregulation of other viral gene products? These are the underlying thoughts guiding the research described in this thesis.

When this project was first started, it was assumed that most of the questions would be answered in the context of recombinant virus studies. In the past decade, rescue of cloned viruses from cDNA has been accomplished for many negative sense RNA viruses from five different families:(1) *Rhabdoviridae*- rabies virus (Schnell *et al.*, 1994), (2) *Paramyxoviridae*- measles virus (Radecke, *et al.*, 1995), mumps virus (Clarke *et al*, 2000), simian virus 5 (He *et al.*, 1997), Newcastle disease virus (Peeters *et al.*, 1999), and HPIV3 (Durbin *et al*, 1997; Hoffman and Banerjee, 1997), (3) *Bunyaviridae* - Bunyamwera virus (Bridgen and Elliott, 1996), (4) *Orthomyxoviridae* - Influenza A virus (Newmann *et al.*, 1999), and (5) *Filoviridae* - Ebola virus (Volchkov *et al.*, 2001). This tool has allowed the introduction of foreign genes, genes from similar viruses, or mutations into the genome of the recombinant viruses (Tao *et al.*, 1998; Sergel *et al.*, 2000; Krishnamurthy *et al.*, 2000; Durbin *et al.*, 2000). Rescue of HPIV3 with different mutations that would increase the expression of functional F protein is one of the ultimate goals of Ken Dimock's lab. However, as a prelude to studying the effects of mutation at the F cleavage site and of the long 5' UTR on F protein expression in a recombinant virus system, they were assessed in a transfection system and *in vitro*.

F. HYPOTHESIS

The goal of this research was to understand the regulation of the HPIV3 fusion protein, F. I rationalized that since there is read-through transcription at the M/F gene junction, since the F mRNA has an unusually long 5'UTR and since only half of the F precursor molecules are cleaved, HPIV3 must need to carefully regulate the amounts of F expressed, and that there must be a reason for these potential regulatory mechanisms to have evolved. Therefore the following hypothesis was formulated;

The amount of functional F protein produced in cells infected by HPIV3 is highly regulated; probably at the levels of transcription, translation and post-translational processing.

G. OBJECTIVES

1- To determine if the long 5' UTR of the F mRNA lowers translation efficiency compared to the other HPIV3 5' UTRs.

2- To determine the effect of altering the F protein furin cleavage site to one that I predict will increase cleavage efficiency; when ^{85}DPRTKR/F^{91} is changed to include an arginine at position -6 relative to the cleavage site, ^{85}RPRTKR/F ^{91}.

3- To construct plasmids and prepare vaccinia stocks in preparation for virus rescue.

II. MATERIALS AND METHODS

A. Cell culture and virology

1. Cells

The human epidermal carcinoma cell line, HEp-2, was provided by Dr. P. Collins at the National Institute of Allergy and Infectious Diseases (NIAID) (National Institutes of Health (NIH), Bethesda, MD). The baby hamster kidney cell line, BHK, was provided by Dr. K. Wright (University of Ottawa, Ottawa, ON). The human epithelial-like cell line, HeLa T4, was obtained from the NIAID AIDS Research and Reference Reagent Program (Rockville, MD). The rhesus monkey kidney cell line, LLC-MK2 was obtained from the American Type Culture Collection (ATCC).

All cell lines were maintained in autoclavable minimal essential medium (MEM) containing Earle salts and supplemented with 10% fetal bovine serum (FBS), 2 mM L-glutamine, 0.225% (w/v) sodium bicarbonate, and 50 μg/mL gentamycin sulfate. Cell monolayers were propagated in 100mm diameter polystyrene dishes (Sarstedt) and grown at 37°C in a 5% CO_2 atmosphere in a Shellab Incubator (Sheldon Manufacturing Inc.)

HEp-2 and HeLa T4 cell monolayers were passaged twice a week at a ratio of 1:10 whereas LLC-MK2 cell monolayers were passaged weekly at a ratio of 1:10. Cells were washed once with 3 mL of prewarmed Tris-buffered saline (TBS; 137 mM NaCl, 5 mM KCl,

0.7 mM Na2HPO4, 5.6mM glucose, 25 mM Tris-Cl pH 7.2). To detach the cell monolayer, 2 mL of 0.05%/0.53mM trypsin-EDTA·4Na in TBS was added and the cells were incubated at 37°C for 5 minutes. The trypsin was inactivated by the addition of fresh medium and cells were diluted into fresh culture plates. All cell culture reagents were obtained from Invitrogen Life Technologies Inc.

2. Viruses

Recombinant vaccinia vTF7-3 expressing bacteriophage T7 RNA polymerase (Fuerst et. al., 1986) was obtained from ATCC. A stock of Modified Vaccinia Ankara expressing the T7 RNA polymerase (MVA-T7) was obtained from Dr. B. Moss (NIAID, NIH, Bethesda, MD). MVA-T7 is a host range mutant of vaccinia whose replication is restricted to avian cell lines and baby hamster kidney cells (Drexler, *et al.*, 1998). This virus can express its proteins in mammalian cells however replication does not occur and the virus disappears after a few passes. A stock of recombinant HPIV3 JS strain was obtained from Dr. M. Skiadopoulos (NIAID, NIH, Bethesda, MD).

3. Preparation of virus stocks

A MVA-T7 stock was prepared as follows. A 70-80% confluent T175 flask of BHK cells was infected at a multiplicity of infection (MOI) of 0.002 plaque forming units (pfu) per cell in a total initial volume of 8 mL. The volume was increased to 20 mL after a 2 hour incubation at 32°C. Cells were monitored for cytopathic effects and were harvested by scraping when the monolayers had a 'lace like' appearance. The cells were dispersed by

pipetting. The supernatant was frozen at -80°C in 2 mL aliquots. Before titration, an MVA-T7 aliquot was re-divided into 100 μL aliquots. Frozen stocks of vTF7-3 and HPIV3 JS were already available.

4. Titration of virus stocks

The MVA-T7 was titrated using end point dilution resulting in the tissue culture infectious dose 50 (TCID50). BHK cells were diluted 1:25 and 50 μL of the cells were seeded in each well of a 96-well plate. A 1:10 dilution of MVA-T7 was added to the first column of BHK cells. 180 μL of MEM was added to each well, 20 μL of the previous dilution was added and mixed by pipetting. On day 5, the wells were observed and the number of infected wells was counted and the dilution corresponding to 50% infectivity was calculated (Reed and Muench, 1938).

B. DNA preparation and analysis

1. Small scale isolation of plasmid DNA (Mini-prep)

All miniprep DNA isolations followed the alkaline lysis method. 3-10 mL of LB broth containing ampicillin (LBA) were inoculated from single *Escherichia coli* colonies or aliquots of frozen bacterial stock, and the culture was incubated on a shaker overnight at 37°C. 1.5-6 mL of the bacterial culture was centrifuged at 13000 rpm for 1 min in microcentrifuge tubes. The supernatant was removed and the cells were resuspended in 150 μL of ice-cold resuspension solution (50mM glucose, 25mM Tris-HCl pH 8.0, 10 mM

EDTA, 100 μg/mL DNAse-free RNAse A. Cells were lysed with 150 μL of fresh lysis solution (1% SDS, 0.2N NaOH) the tubes were inverted 4-5 times and the solution became clear and viscous. The solution was neutralized with 150 μL of ice-cold neutralization solution (5M potassium acetate pH 4.8) and mixed gently resulting in the loss of viscosity and the formation of a large white precipitate. The samples were centrifuged at 4°C at maximum speed for 5 min. The supernatant was transferred to a fresh microfuge tube and incubated at 37°C for 10-20 min to eliminate the RNA. Following this step, either a "crude" or a "purified" plasmid preparation was followed. The "crude" DNA samples were used for routine plasmid screening and the "purified" DNA was used for transfections or mutagenesis reactions.

a) Crude preparation: The supernatant was extracted with 400 μL of chloroform and 1 mL of cold ethanol was added to precipitate the DNA. After a short -20°C incubation, the DNA was precipitated by centrifugation at 4°C for 10 min. The ethanol was removed and the pellet was resuspended in 40 μL ddH_2O.

b) Purified preparation: 1 mL of Wizard® resin or 500 μL of diatomatous earth (DE) resin (Kim and Pallaghy, 1996) was added to the supernatant and the resin was collected on a Wizard® mini-prep column by vacuum filtration. The column was washed with 2 mL of 80% isopropanol or 2 mL of Column Wash (95% ethanol). The DNA was eluted from the column with 50 μL ddH_2O by centrifugation. For sequencing, the DNA was precipitated by adding 2M NaCl to a final concentration of 0.1M and 2.5 volumes of ethanol. Precipitation

was carried out overnight at -20°C. The DNA was pelleted by centrifugation at maximum speed at 4°C for 20 min.

2. Large scale plasmid DNA isolation (Midi-Prep)

50-100 mL of LBA was inoculated from an aliquot of frozen bacterial stock and incubated overnight on a shaker at 37°C. The bacterial cells were pelleted by centrifugation in 250 mL bottles at 6500xg for 10 min at 4°C. The cells were resuspended in 3 mL resuspension solution in a Corex tube. The cells were lysed with 3 mL lysis solution and gently rotated the solution. The lysate was neutralized by adding 3 mL of neutralization solution and was gently rotated so as not to shear the genomic DNA. The corex tube was centrifuged at 13000xg for 30 min at 4°C. The supernatant was transferred to a 50 mL conical tube and incubated at 37°C for 20 min. A disc of 3mm filter paper was cut and plunged into place in a 10 mL syringe. 10 mL of DE resin was added to the supernatant and the mixture was pulled through the syringe by vacuum. The column was washed 3 times with 10 mL of column wash (95% EtOH). The tip of the syringe was placed over a 1.5 mL microfuge tube and placed in a 50 mL conical tube and centrifuged in a swinging bucket centrifuge (Sorvall, GLC-2B) for 2 min at 1500rpm. The DNA was eluted with 2 x 500 mL ddH_2O in the same fashion.

3. Agarose gel electrophoresis

DNA electrophoresis was performed in 1% agarose gels in 1X Tris-Acetate buffer (TAE; 40 mM Tris-acetate, 1mM EDTA, pH 8.0). Samples were prepared by adding 10X

loading buffer (60% glycerol, 50mM Tris pH 7.6, 0.25% bromophenol blue, 0.25% xylene cyanol) at a ratio of approximately 1:10. Electrophoresis was carried out in a Horizon 58 (Gibco/BRL) apparatus was used for electrophoresis at approximately 10 volts/cm. To stain DNA, gels were incubated in TAE buffer containing 1 μg/mL ethidium bromide. Gels were destained in H_2O. Photography was performed using an AlphaEase™ imager with a U.V. light box (Alpha Innotech Corporation).

4. DNA sequence analysis

Automated fluorescent sequencing was performed by the Biotechnology Research Institute of the University of Ottawa (UOBRI).

C. RNA preparation and analysis

1. *In vitro* transcription

The pKSCAT plasmid DNA templates for *in vitro* transcription was linearized by restriction enzyme digest with HindIII. Samples were deproteinized by phenol/chloroform extraction and chloroform extraction and DNA precipitated overnight at -20°C with ethanol. The *in vitro* transcription recipe for one 25μL reaction was 5μL of 5X *in vitro* transcription buffer, 2.5μL of 100mM DTT, 2.5 μL of each 10mM ATP, GTP, CTP, UTP and 1 μL RNA guard (40U), this mixture was warmed to 37°C and then 75 ng of linearized and diluted pKSCAT plasmid and 60 U of T7 RNA polymerase were added. The mixture was incubated overnight at 37°C and frozen at -20°C.

2. RNA agarose gel electrophoresis

A stock of H_2O was treated with diethylpyrocarbonate (DEPC) by adding 0.1-0.2mL DEPC per 100mL H_2O. The solution was incubated overnight and then autoclaved to remove any remaining DEPC. A Horizon 58 (Gibco/BRL) apparatus was soaked in a 0.1-0.2% SDS solution to remove any ribonucleases (RNAses) and then rinsed with DEPC treated H_2O. A 1X TAE solution was made RNAse free using DEPC treated H_2O and 25X TAE stock. A stock of 1% Agarose in 1X TAE was also prepared using DEPC treated H_2O. All solutions were autoclaved. The RNA samples were kept on ice and prepared by adding 10X RNA loading buffer (50% glycerol, 1mM Na_2EDTA and 0.4% bromophenol blue) in a 1:10 dilution. The rest of the protocol was as described in the section on DNA agarose gel electrophoresis.

3. *In vitro* translation of RNA

A Flexi® Rabbit Reticulocyte Lysate System by Promega was used for *in vitro* translation according to the manufacturer's specifications. Each 25 μL sample contained 0.25μL of amino acid mixture minus leucine (1mM), 0.25μL the amino acid mixture minus methionine (1mM), 1μL of magnesium acetate (25mM) and 0.7μL of potassium chloride (2.5M). 1μL of a 1:20 dilution of luciferase RNA was used as an internal control. No DTT was added to the reaction. To avoid variation, aliquots from a common reaction mixture were used for the translation of all mRNAs in a given experiment. 250 ng of RNA template was denatured at 65°C for 3 min and added to each sample. The reaction was incubated for 90 minutes at 30°C. The translation mix was frozen at -20°C.

4. Chloramphenicol acetyl transferase enzyme linked immunosorbent assay (ELISA)

The CAT ELISA kit from Roche was used to detect CAT protein according to the manufacturer's specifications. 5 μL of the *in vitro* translation mix was mixed with 195 μL of ELISA sample buffer. After the addition of the ABTS substrate solution, the absorbance of the samples was measured in a microtiter plate reader at 405nm with a reference wavelength of 492nm.

5. Luciferase assay

Each *in vitro* translation mixture was diluted 1:1000 and between 1 and 5 μL of the dilution was placed in a microfuge tube. Each sample was mixed with Luciferase assay reagent (LAR) to a final volume of 25 μL and placed in a scintillation counter (LKB Wallac, 1214 RACKBETA liquid scintillation counter). Each sample was counted for chemiluminescence for 60s. The total number of counts was determined after subtracting the counts from a blank tube without luciferase. On one occasion, the liquid scintillation counter was not operational, so I used a luminometer (Junior LB 9509, Berthold technologies).

6. Analysis of the Free Energy of the RNA

The sequence of the 5' UTRs were analysed for hairpin structures by using the online software: IDT Biotools OligoAnalyzer 3.0. The web address for this tool is: http://207.32.43.70/biotools/oligocalc/oligocalc.asp

D. Restriction and modification enzymes

Restriction endonucleases were purchased from New England Biolabs, Promega Biotech, Amersham Biosciences, Pharmacia Canada, Gibco/Life Technologies, Epicenter Technologies and Ambion. Restriction and modification enzymes were used as recommended by the suppliers.

Ligations were performed by mixing vector and insert in a ration of 1:5 based on mass in a final volume of 50 μL. 5X buffer and T4 DNA ligase were purchased from New England Biolabs. The reaction was carried out overnight at 4°C.

E. Purification of DNA restriction fragments from agarose gels

DNA fragments to be cloned were purified from 1% low melt agarose gels by cutting the gel approximately 30 cm away from the UV light source to avoid damaging the DNA. The agarose band was then heated to 70°C to melt the agarose and 1 mL of Wizard DNA purification resin or DE resin was added to the gel. The DNA was purified as described in the section on small scale isolation of plasmid DNA (miniprep).

F. Construction of pIBIJS-F-flag and pIBIJS-F*-flag

The plasmid pIBIJS-F was provided to me by Reza Nokhbeh. He constructed it by

removing the HPIV3 Washington 57 F coding sequence from the pIBI vector and inserting the HPIV3 JS F coding sequence. It was important for all of these studies to be carried out on HPIV3 JS because this is the strain that we will eventually be rescuing.

1. Mutagenesis of pIBIJS-F

pIBIJS-F plasmid DNA was isolated from an overnight culture using the miniprep protocol described in the DNA preparation section. Two primers were designed for mutagenesis of the furin cleavage site: F-furin mut (+): tcc aat gaa aac act **cg**t ccc aga aca aaa cg and F-furin mut (-): cgt ttt gtt ctg gga **cg**a gtg ttt tca ttg ga. Both primers were resuspended in ddH_2O to 1 μg/μL then diluted 1:100 to a final concentration of 10 ng/μL. Mutagenesis of 100 ng of pIBIJS-F in a 50 μL reaction was as follows: 5 μL of 10X PFU turbo polymerase reaction buffer (200mM Tris-HCl pH8.8, 20mM $MgSO_4$, 100mM KCl, 100mM $(NH_4)_2SO_4$, 1% Triton, 1mg/mL nuclease-free BSA), 100 ng pIBIJS-F, 125 ng of both F-furin mut (+) and F-furin mut (-), 200 μmol dNTP and 2.5 U PFU turbo polymerase. The mutagenesis was carried out in a Techne thermocycler with the following program: 1. 1 cycle at 95°C for 1 min, 2. 19 cycles at 95°C for 50 s, then at 55°C for 1 min, then 68°C for 10 min (2 min/ kb template), 3. 1 cycle at 68°C for 7 min, 4. overnight at 4°C. The DNA was digested with 6 U of DpnI for 1.5 hrs at 37°C, to degrade parental, methylated plasmid DNA. The mixture was extracted with chloroform and the DNA was precipitated in 2.5 volumes of ethanol overnight at -20°C. The DNA was resuspended in10 μL of ddH_2O. The sample was heated to 95°C and allowed to slowly cool to room temperature so that the plasmid DNA would recircularize.

2. Electroporation

1-2 μL of mutagenized DNA was mixed with 20 μL of Top10 *E. coli* cells that had been washed of salt and stored in 10% glycerol. The mixture was placed in a sterile cuvette in the electroporation chamber. Conditions for electroporation were as follows: resistance = 4 kΩ, capacitance = 330μF, resistance of medium = low. 0.5 mL of SOC medium (2% tryptone, 0.5% yeast extract, 0.05% NaCl supplemented with 10mM $MgSO_4$ and 20mM glucose) was added to the cells after electroporation and cells were incubated for 1 hour at 37°C. A 100 μL and 400μL aliquot of cells were plated on LBA agar plates (1% typtone, 0.5% yeast extract, 0.5% NaCl, 150 μg/mL ampicillin) and the plates were incubated at 37°C overnight. Colonies were picked for inoculation of liquid cultures in 3mL LBA.

3. Screening for furin cleavage mutants of pIBIJS-F

A primer was designed for screening potential mutants by sequence analysis; JSF930: ccg ctg taa ttt gtg ctg ag. The DNA from 24 clones was digested and analysed by agarose gel electrophoresis to ensure that it was the correct size. Twelve candidate DNA samples, that appeared to be the correct size and digestion pattern, were purified as described in the section of small scale isolation of plasmid DNA (miniprep), and were manually sequenced by Reza Nokbeh. The sequence of the clone chosen was subsequently confirmed by automated sequencing (UOBRI). The clone was named pIBIJS-F*.

4. FLAG tagging both pIBIJS-F and pIBIJS-F*

The F gene from the HPIV3 WASH57 had been previously FLAG-tagged in pIBIF70.

The following primers were created to PCR amplify the FLAG tagged region of pIBIF70: FNdeflag(+): caa aag aga aat cga gtg gat c and FBamH1flag (-): cta aag gga gag aat tcg agc. The following conditions were used for the 50 μL PCR reaction: 5 μL of 10X pfu reaction buffer (200mM Tris-HCl pH8.8, 20mM MgSO4, 100mM Kcl, 100mM (NH4)2SO4, 1% Triton, 1mg/mL nuclease-free BSA), 18 ng of pIBIF70, 10 pM of FNdeflag(+) and FBamH1flag (-), 200 μmol dNTP and 2.5 U PFU turbo polymerase. The PCR was carried out in a Techne thermocycler with the following program: 1. 1 cycle at 95°C for 1 min, 2. 30 cycles at 95°C for 50 s, then at 55°C for 1 min, then 68°C for 45s, 3. 1 cycle at 68°C for 7 min, 4. overnight at 4°C. pIBIJS-F, pIBIJS-F* and the amplification product were digested first with BamH1 and the samples were extracted with chloroform. The DNA was precipitated overnight at -20°C with ethanol. The DNA was then digested with NdeI and the sample was heated for 20 min at 65°C. The BamH1/NdeI plasmid fragments were gel purified, as described above, and ligated with the PCR fragment in a total volume of 20 μL with 3-4 U of T4 DNA ligase, overnight at 4°C. The ligation products were used to transform *E. coli*, colonies were picked and plasmid DNA was isolated from liquid cultures. Plasmid DNA was screened by BglII digestion and agarose gel electrophoresis. The flag tag generates an extra BglII site in the pIBIJS-F constructs (fragment sizes 4053 bp, 520bp and 250bp instead of 4303 bp and 520 bp). The sequence of the constructs was confirmed by automated sequencing (UOBRI).

G. Protein analysis

1. Transfection

For transfections, HeLaT4 cells were grown to ~90% confluency in 6-well dishes. Generally, transfection mixes contained 100 ng of pIBIJS-F-flag or pIBIJS-F*-flag alone or with 1000 ng of pCITEHN-flag and a control plasmid, pCR2.1TOPO. For each well, the transfection reagent Lipofectin (Invitrogen) was diluted to 2% in 100 μL Optimem (Invitrogen), and the mixture was incubated for 30 min at room temperature. For each well, plasmid DNA was diluted in 100 μL Optimem, combined with 100 μL of the Lipofectin/Optimem mixture, and incubated at room temperature for 30 min. 200 μL of the transfection mixture was combined with vTF7-3 (MOI = 10), the final volume was adjusted to 750 μL with Optimem and the complete transfection mixture was added to cells that had been washed once with TBS. Cells were incubated at 37°C for 5 hours and 750 μL of fresh medium containing 10% FBS and 80μg/mL cytosine arabinoside hydrochloride (ara C, Aldrich) and was added to each well. Cells were incubated overnight at 37°C.

2. Preparation of cell lysates

Transfected cells were scraped from wells with a cell scraper and pelleted in microfuge tubes at 4000 rpm at room temperature for 2 min. Supernatants were removed by gentle suction and cells were lysed on ice in 150 μL of 0.5% SDS (BDH) in Optimem containing 1mM phenylmethylsulfonyl fluoride (PMSF, Sigma). Lysates were sonicated using a high power probe to reduce viscosity and were stored at -80°C.

3. Polyacrylamide gel electrophoresis (PAGE)

Protein analysis was carried out by electrophoresis in 9% polyacrylamide gels containing SDS (SDS-PAGE) under reducing conditions using the BIO-RAD Mini-PROTEAN II system. The separating gel was composed of 9% acrylamide, 0.3% bis-acrylamide, 0.1% SDS and 750 mM Tris-HCl, pH 8.8. The stacking gel was composed of 5% acrylamide, 0.13% bis-acrylamide, 0.1% SDS and 66 mM Tris-HCl, pH 6.8. Both gels were polymerized using 0.1% ammonium peroxodisulphate (BDH) and a 1/1000 dilution of TEMED (NNN'N'-tetremethylethylenediamine, BIO-RAD). Prestained broad range protein markers (NEB) were used to estimate molecular mass. All samples were prepared by adding one-quarter volume of 4X SDS-PAGE sample buffer (11% glycerol, 62mM Tris pH 6.8, 2.2% SDS, 0.1% Bromophenol blue and 20% β-mercaptoethanol) and heating to 95°C for 5-10 minutes. Electrophoresis was carried out in electrophoresis buffer solution (25 mM Tris base, 192 mM glycine and 0.1% SDS) at 50 volts for approximately 3 hours (until the bromophenol blue dye front ran off the gels).

4. Western blot analysis

Proteins were transferred from SDS-PAGE gels onto PVDF (polyvinylidene fluoride, Millipore) membranes overnight at 4°C at 30 V in transfer buffer (192 mM glycine, 25 mM Tris base, 20% Methanol) using the Bio-RAD Mini Trans-Blot cell. The membrane was removed from the transfer apparatus, washed twice in a small amount of TBS for western blots (0.075M NaCl and 0.01M TRIS pH 7.5) and rocked for 5 min at room temperature. Each membrane was blocked in 7-8 mL of TBS-3% BSA for 1 hour at room temperature,

with rocking. The membrane was then washed twice in 15 mL of TBS Tween-Triton (0.25M NaCl, 0.02M TRIS pH 7.5, 0.002% v/v Triton X-100 and 0.0005% v/v Tween-20) and once in TBS. The membrane was then incubated in mouse anti-FLAG M2 monoclonal antibody (Sigma) diluted 1:10 000 in TBS-3% BSA for 40 min at room temperature. The three washes were repeated and the membrane was then incubated for 1 hour at room temperature in the secondary antibody, rabbit anti-mouse IgG/ conjugated with horseradish peroxidase, freshly diluted 1:7500 in TBS-3% BSA. The membrane was then washed three times in TBS-Tween-Triton, placed in the developing solution (solution A: 2.5 mM luminol and 0.396 mM p-cumeric acid in 0.01M TRIS pH 8.5 solution B: 0.54mM H_2O_2 in 0.01M TRIS pH 8.5) for 1 min and exposed for various amounts of time to film (Cronex film, Dupont). Film developed in a KODAK X-OMAT 2000A processor.

H. Analysis of gels:

1. Densitometry

RNA and DNA gels, and Western Blot films were photographed using the Alpha Ease Imager and the photos were stored digitally on a computer. The images were then subjected to spot densitometry analysis using the AlphaEase™ software version 3.3b_gc (Alpha Innotech Corporation). Whenever possible with the RNA and DNA gels, the MassRuler™ DNA ladder mix (MBI Fermentas) was used to plot a calibration curve and the amount of RNA or DNA was established relative to this curve or relative to another sample of RNA or DNA.

I. Analysis of Fusion

Certain notes should be made for the two fusion assays described below. Prior to each transfection experiment, to verify that the quantities of pIBIJSF-flag and pIBIJSF*-flag transfected into cells were identical, plasmid DNA was electrophoresed on a 1% agarose gel and the quantity of DNA was measured against a ladder in which each band has a specific quantity of DNA. When two experiments were carried out on the same day, the dilution series for each was prepared independently. Finally, each experiment was performed in duplicate and each well of the assay was analysed twice by spectrophotometry, to ensure that any minor variations were accounted for. The only caveat is that throughout the experiments, only one preparation of pIBIJSF*-flag and pIBIJSF-flag as well as pCITEHN-flag DNA plasmids were used. However, all the proteins produced were functional and the correct size as determined by Western Blot analysis.

1. Qualitative fusion assay

HeLaT4 cells in a 24-well dish were transfected with plasmid DNA. Generally two series of dilutions were performed were performed. The samples in one series contained 3.125ng, 6.25ng, 12.5ng, 25 ng, 50ng and 100ng of pIBIJS-F-flag or pIBIJS-F*-flag DNA, together with 250 ng of pCITEHN-flag DNA (in each sample). Samples in the second series contained 250ng, 25ng, 2.5ng, 1.125ng and 0.25ng of pIBIJS-F-flag or pIBIJS-F*-flag DNA, together with 250 ng of pCITEHN-flag. Negative controls samples were: (1) 250ng of pCITEHN-flag alone, (2) 25 ng of pIBIJS-F-flag or (3) 25 ng of pIBIJS-F*-flag. Lipofectin

(Invitrogen) was diluted to 2% in Optimem (Invitrogen), 12.5 μL per well, and incubated for 30 min at room temperature. Plasmid DNA diluted in 12.5 μL Optimem per well was combined with an equal volume of the Lipofectin/Optimem mixture and incubated at room temperature for 30 min. VTF7-3 (MOI = 3) and Optimem were added to adjust the final volume of each transfection mixture to 225 μL. The cells were incubated at 37°C for 3-5 hours with transfection mixes and then an equal volume of fresh medium containing 10% FBS and 80 μg/mL araC was added. Cells were incubated overnight at 32°C and examined visually under the microscope.

The cells were then assessed visually under the microscope and the number and size of syncytia were evaluated. This qualitative fusion assay, however, is subject to observer bias, and the results obtained by counting syncytia per microscope field are always approximate. Therefore, all samples were evaluated by me and by at least one other observer who was "blind" to the sample order.

2. Quantitative fusion assay (Nussbaum *et al.*, 1994)

HeLaT4 cells in a 24-well dish were prepared and transfected with plasmids encoding F and HN, exactly as described for the qualitative fusion assay except that 2 mU/mL of *Vibrio cholerae* neuraminidase (Roche) were added prior to the overnight incubation to prevent syncytium formation. A 100 mm culture of HeLa T4 cells was washed twice with 4 mL Optimem and then transfected with plasmid pG1N-T7βgal. pG1N-T7βgal contains the β-galactosidase (β-gal) gene under control of the T7 RNA polymerase promoter. For

transfection, 12 μL of Lipofectin was added to 500 μL of Optimem and incubated at room temperature for 30 min. 6 μg of pG1N-T7βgal was added and the mixture was incubated an additional 30 min at room temperature. 250 μL of vaccinia WR was added to the DNA/Lipofectin mixture and the final volume was brought to 3.25 mL with Optimem. Cells were transfected at 37° C for 3-5 hours. The transfection mix was removed and the cells were washed with Optimem. The cells were trypsinized and pelleted and the pellet was washed twice with 4 mL TBS. The cells were resuspended in 4 mL Optimem and incubated overnight at 32°C.

HeLa T4 cells transfected with pG1N-T7β-gal were washed twice in TBS and resuspended in 2.5 mL of Optimem containing 2% FBS and 40 μg/mL of Ara C. The cells in the 24-well dish were washed twice very gently with Optimem and overlaid with100 μL per well of pG1N-T7β-gal transfected cells. The cells were incubated at 37°C for 3 hours then lysed *in situ* by adding 8 μL of 10% NP40. Lysates were frozen *in situ* at -80°C. 25 μL of each lysate was mixed with an equal volume of CPRG (chlorophenol red-β-D-galactopyranoside monosodium salt, Roche) (16mM CPRG, 120mM Na_2HPO_4, 80mM NaH_2PO_4-$8H_2O$, 20mM KCl, 2mM $MgSO_4$, 1mM β-mercaptoethanol) in a 96-well microtiter plate and the absorbance was read at 574nm for 40 min at 5 min intervals.

3. Flow Cytometry (see Appendix)

HeLa T4 cells in a 6-well dish were transfected with either 1 μg of pCITEHN (negative control) or with 1 μg pCITEHN and 100 ng of pIBIJSF-flag. Cells were infected

with VTF7-3 (MOI = 5-10) and the final transfection volume was brought to 600 μL. Cells were incubated at 37°C for 6-7 hours, washed with TBS and trypsinized in 0.5 mL. The cells were pipetted up and down to yield a monocellular suspension. 0.5 mL of PBS (137mM NaCl, 2.7 mM Kcl, 4.3 mM Na_2HPO_4 and 1.4mM KH_2PO_4) was added and cells were pelleted in microfuge tubes at 3000 rpm, at room temperature. The cells were washed in PBS, resuspended by vortexing in a small amount of the supernatant and 1 mL of ice-cold 70% ethanol was added drop by drop to the cells, with vortexing. Cells were incubated at 4°C overnight.

The fixed cells were pelleted at 3000 rpm in a microcentrifuge for 5 min at room temperature. Most of the ethanol was removed, the cells were resuspended in 0.5 mL of PBS containing 1 mg/mL RNAse A, and incubated while rocking for 30 min at room temperature. The cells were pelleted and the supernatant was removed. Each cell pellet was resuspended in 1 mL of PBS and divided into two 5 mL polypropylene tubes. An additional 0.5 mL of PBS was added to each tube and 25 μL of a 1mg/mL propidium iodide solution was added to one tube of each pair. The cells were incubated at 4°C for 15 minutes and then analysed by flow cytometry (Coulter EPICS XL-MCL, Beckmann Coulter).

J. Preparation of plasmid constructs for rescue

1. Introduction of unique *Sbf* I site

The antigenome of HPIV3 is vectored in an 18 Kb plasmid, provided to us by

Skiadopoulous and Murphy (NIH), named p3/7(131)2G+ which I will call p2G (Durbin *et al.*, 1997). The part of the HPIV3 genome that would be targeted for these experiments is from the 3' end of the M gene to the cleavage site in the F gene, but does not have any unique restriction sites that would render cloning easy. In Figure 4, this region of the HPIV3 genome and the modifications that were made are represented in the various plasmid backgrounds. Therefore, the first step was to modify the *Pst* I site at 4372 nt (refers to the position in the HPIV3 JS genome) to a unique *Sbf* I site without changing the amino acid coding. This *Sbf* I site would then allow me to mutate the region of interest in a small plasmid such as pCR2.1topo and then move the small *Sbf* I - *Bst* EII fragment into the large p2G. Therefore, a segment of p2G between the restriction sites *Nco* I and *Bst* EII was amplified by PCR and cloned into pCR2.1Topo to create the pCR2.1 Topo Bst-Nco plasmid. Two complementary mutagenic primers (each one anneals to different strands of the parental plasmid) were used to introduce the unique *Sbf* I site into that plasmid and to create pCR2.1TopoBst-Nco-Sbf. The *Nco* I site is not unique, there is one other site in the L gene, therefore in order to move the new mutation into the full length antigenomic plasmid, an intermediate step needed to be performed. p2G-Hpa is a plasmid that is the result of digestion of p2G with the restriction endonuclease *Hpa* I (cuts the p2G plasmid twice, once at the end of the F gene and once in the L gene) and religation of the large plasmid. This removes the second *Nco* I site, at 8195 nt, from the L gene and renders the *Nco* I, at 4170 nt, unique in p2G-Hpa. p2G-Sbf was created following the introduction of the unique *Sbf* I site in p2G-Hpa by simple cloning, the p2G-Hpa-Sbf was digested at the unique restriction sites *NgoM* IV and *Bst* EII and ligated to the vector containing *NgoM*IV-*Bst* EII fragment of p2G.

Figure 4 **Schematic representations of the plasmid constructs for HPIV3 rescue.** The names of each of the plasmids are on the left of each diagram. There are two pCR2.1Topo plasmids named pCR2.1Topo Nco-BstEII and pCR2.1Topo Rsr-SwaI. The numbers at the end of each plasmid corresponds to the length of that plasmid. p2G-Hpa was created by digesting p2G with HpaI and religating it, this causes the NcoI site in the M gene to be unique and allows easy movement of the Sbf I mutation into the new plasmid p2G-Hpa-Sbf. p2G-sbf can then be created by moving the BstEII - NgoMIV fragment into the p2G.

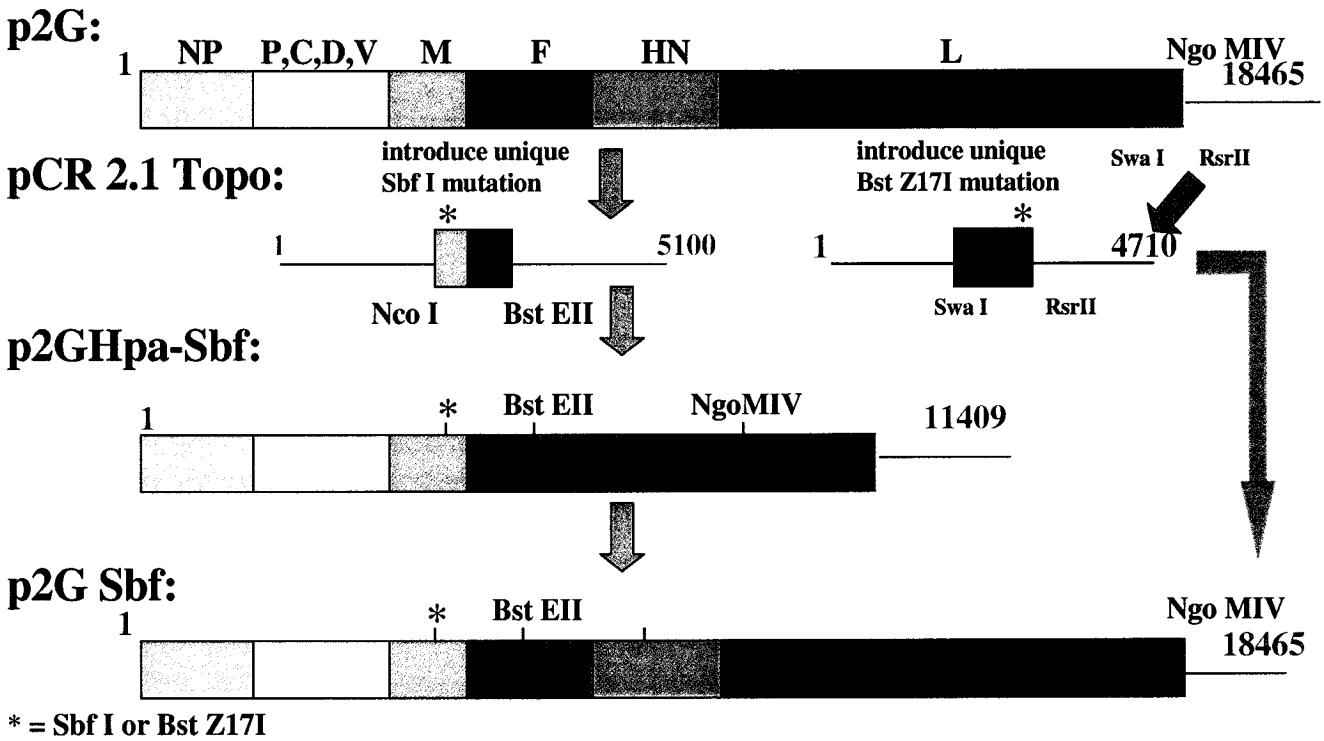
p2G:
1
NP
P,C,D,V
M
F
HN
L
Ngo MIV
18465
pCR 2.1 Topo:
introduce unique
Sbf I mutation
*
1
5100
Nco I
Bst EII
introduce unique
Bst Z17I mutation
Swa I
RsrII
*
1
4710
Swa I
RsrII
p2GHpa-Sbf:
1
*
Bst EII
NgoMIV
11409
p2G Sbf:
1
*
Bst EII
Ngo MIV
18465
* = Sbf I or Bst Z17I

2. Removal of the 8 extra nucleotides

One of the interesting experiments to be carried out in a rescue system would be to remove the 8 extra nucleotides at the M-F gene junction that cause transcriptional readthrough. This phenomenon decreases the amount of F mRNA that is available to be translated. An interesting question to ask would be what happens to the virus if the amount of F is increased. Therefore, a construct is necessary to be able to move that deletion into p2G. I took the pCR2.1TopoBst-Nco-Sbf and utilized the 2 primer method to delete the 8 nucleotides at the M-F gene junction (Figure 5), this construct has yet to be moved into a p2G with an adjusted register of +2 (See below).

3. Introduction of unique *Bst* Z17 site

The paramyxoviruses adhere to the "rule of 6" ie. their genomes are always exact multiples of 6 nucleotides because that is the number of nucleotides calculated to be covered by one NP molecule (Kolakofsky *et al.*, 1998). Due to this rule, if any mutations are introduced that change the number of nucleotides in the genome to something other than a multiple of 6, then the register of the genome needs to be adjusted, otherwise nucleotides at the 3' end of the genome or antigenome are thought to be removed by nucleases. Genomes that are not 6n nucleotides in length modify the location of the promoter element in relation to the terminal N subunit and are accordingly poorly initiated (Kolakofsky et al., 1998). One place to adjust the register of the genome (without affecting coding) is between the L translation termination codon, before the L 3' UTR. This addition was shown to have no affect on the functioning of the minigenome system (Jogalakar, 2000). I decided to introduce

Figure 5 **Schematic representations of the plasmid constructs for rescue of HPIV3 with a modified M/F gene junction.** The names of each of the plasmids are on the left of each diagram. Only the two pCR2.1Topo plasmid have been constructed, the final plasmid is the eventual end product. The numbers at the end of each plasmid corresponds to the length of that plasmid.

pCR 2.1 Topo-Sbf:

deletion of M/F 8 extra nucleotides

pCR 2.1 Topo-Sbf M/Fmut -8:

2G Sbf BstZ17 +2-M/F mut-8:

*** = Sbf I**

a unique *Bst* Z17 site (Figure 4), which would make it easy to detect any additional mutations that destroy the site. The *Bst* Z17 restriction endonuclease is a 6 base cutter which means that the addition of the site will follow the rule of 6. The new construct generated with the addition of the *Bst* Z17 site will be the control construct in the rescues. A fragment in p2G between the unique restriction sites *Rsr* II and *Swa* I was amplified by pcr and cloned into the pCR2.1 Topo vector and the new construct was named pCR2.1TopoRsr-Swa. Again two complementary mutagenic primers (each one anneals to different strands of the parental plasmid) were used to introduce the unique *Bst* Z17 site into that plasmid and to create pCR2.1TopoRsr-Swa-BstZ17.

III. RESULTS

The overall objective of this research was to understand the regulation of the HPIV3 fusion protein, F. There are at least three methods that the virus could employ to regulate the amount of functional fusion protein present in infected cells and on the surface of virions. The first method is transcriptional regulation. The second method is translational regulation by the 5' UTR and the third is post-translational modification of the protein. The last two methods will be the focus of this thesis.

A. Translational regulation

It is possible that regulation of fusion protein expression is due to the fact that the mRNA encoding the fusion protein has a 5' UTR that is longer than that of the other mRNAs. This may cause the ribosome difficulty or perhaps slow down the rate of translation of the F message. To further investigate this hypothesis, Justin Rouselle (Rouselle, unpublished) constructed a series of plasmids containing the chloramphenicol acetyl transferase (CAT) open reading frame downstream of the 5' UTR of each of the viral mRNAs (Table 1). This way the relative efficiency of translation for each 5' UTR could be determined and compared.

Each 5' UTR was sequenced as was the entire CAT coding sequence of pKSCAT-M and pKSCAT-F. The pKSCAT-F construct originally had two mutations in the 5' terminus of the CAT coding sequence. A primer was designed to repair both mutations and 20

Table 1: PKS plasmids containing different HPIV3 5' UTRs.

The name of the plasmid containing the 5' UTR[1]	length of the 5' UTR	The sequence of the 5' UTR [2]
pKSCAT-N	45	aca ttg act aga agg tca aga aaa ggg aac tct ata att tca aaa
pKSCAT-P	69	aat cct atc ata cca gaa cat aga gtg gta aat tta gag tct gct tgc aac tca atc aat aga gag ttg
pKSCAT-C	79	aat cct atc ata cca gaa cat aga gtg gta aat tta gag tct gct tgc aac tca atc aat aga gag ttg atg gaa agc g
pKSCAT-M	22	aat aaa tta atc ctt gtc caa a
pKSCAT-F	192	aag tca ata cca aca act att agc agc cac act cgc tgg aac aag aaa gaa ggg ata aaa aaa gtt taa cag aag aaa caa aaa caa aaa gca cag aac acc aga aca aca aga tca aaa cac cca acc cac tca aaa cga aaa tct caa aag aga ttg gca aca caa caa aca ctg aac atc cca acc cac tca aaa cga aaa tct caa aag aga ttg gca aca caa caa aca ctg aac atc
pKSCAT-HN	63	tta cgc aat tca act cta ctc ata taa ttg aga aag aac cca aca gac aaa tcc aaa tcc gag
pKSCAT-L	12	cat gct cga aaa

[1] the name of the plasmid incorporates the name of the HPIV3 gene containing the 5'UTR
[2] putative upstream ATGs are underlined

possible repaired mutants were selected but never screened to ensure that the mutations had been corrected (Rouselle, unpublished). Therefore, I undertook the screening of each of these plasmids for CAT expression in a mammalian transfection system. Each plasmid was purified using DE resin and transfected into HeLaT4 cells in a 24 well dish using VTF7-3 and lipofectin. The cells were incubated overnight and were lysed using a solution containing 0.1% NP40 and 1mM PMSF in Optimem media. These lysates were subjected to a CAT ELISA. Table 2 shows that 15 of the 20 pKSCAT-F repair clones were positive for CAT expression. The clones pKSCAT-5, 6 and 7 were chosen for sequencing. pKSCAT-F6 contained no mutations and is the pKSCAT-F clone that was used for the remainder of the experiments.

Once it was determined that CAT protein was being expressed, the system needed to be optimized to ensure that the *in vitro* translation system was not being saturated with the RNA. Also it was necessary to ensure that we were not at the limit of colorimetric detection of CAT and within the dynamic range of the spectrophotometer. The first thing that needed to be determined was the range of RNA that could be used in the *in vitro* translation to produce CAT. In a preliminary experiment, 1 μL of undiluted pKSCAT-M, the plasmid with the 5' UTR of the HPIV3 M mRNA upstream of the CAT coding sequence, transcript had been used in the *in vitro* translation mix. When 10 μL of this *in vitro* translation reaction was used in the CAT ELISA, the colour change had been extraordinarily rapid. Therefore, it was decided to test a series of RNA dilutions; using 1 μL of 1:5 to 1:160 dilutions of the RNA in the *in vitro* translation mix. Different amounts of each *in vitro* translation reaction

Table 2: CAT expression of pKSCAT-F repair clones.

pKSCAT-F clone	CAT expression[1]	pKSCAT-F clone	CAT expression	pKSCAT-F clone	CAT expression
F1	(-)	F8	(-)	F15	(+)
F2	(-)	F9	(+)	F16	(-)
F3	(+)	F10	(+)	F17	(+)
F4	(+)	F11	(+)	F18	(+)
F5	(+)	F12	(+)	F19	(-)
F6	(+)	F13	(+)	F20	(-)
F7	(+)	F14	(-)		

[1] (-) denotes no CAT expression; (+) denotes CAT expression. The original pKSCAT-F plasmid did not express CAT due to a mutation in the CAT coding sequence, this table indicates which of the twenty repair clones expressed CAT.

were also applied to the CAT ELISA to determine the limits of CAT detection. 5 μL of undiluted *in vitro* translation reaction or 5 μL of a 1:5 dilution or a 1:10 dilution of the *in vitro* translation mix was used for the CAT ELISA. The only dilution that was detected in the ELISA reaction was the undiluted *in vitro* translation mix with the 1:5 dilution of the RNA. The concentration of CAT was determined to be 0.188 ng/mL according to the calibration curve of absorbance versus concentration of CAT in ng/mL.

In another series of preliminary experiments with pKSCAT-M RNA,125ng, 500ng and 1000ng were tested in the *in vitro* translation system. To determine the amount of the *in vitro* translation reaction that should be added to the CAT ELISA, 5μL of undiluted rabbit reticulocyte lysate (Figure 6), and 5μL of a 1:5, 1:10 and a 1:20 dilution of the *in vitro* translation mixes were added. The results showed that the amount of CAT detected when 1:10 and 1:20 dilutions of *in vitro* translation mix were used (at all amounts of RNA) was too weak to be used in a quantitative assay (data not shown). Both 5μL of undiluted and 5μL of a 1:5 dilution of *in vitro* translation mix gave signals, however the signal with the undiluted *in vitro* translation mix was the strongest. These results also suggested that using 5μL of undiluted *in vitro* translation mix containing 250ng of RNA would not saturate the reticulocyte lysate system nor the colourimetric detection (Figure 6). These data were reconfirmed by performing the same experiment using 125ng, 250ng and 375ng of pKSCAT-M RNA. It was also decided to include 50 ng of luciferase mRNA in each translation reaction to control for the potential differences in transcript purity and to allow for normalization, if necessary. This experiment was also designed to determine the

Figure 6 **Optimization of the *in vitro* translation system and the CAT ELISA.** Different quantities of *in vitro* transcription mix were translated *in vitro* and then different dilutions of the *in vitro* translation mix were assayed in the CAT ELISA. The results in this figure were those for 125, 500 and 1000 ng of undiluted *in vitro* transcription mix translated *in vitro*. 5 μL of these *in vitro* translations were assayed undiluted in the CAT ELISA. This graph is the absorbance at 405 nm versus time in the CAT ELISA.

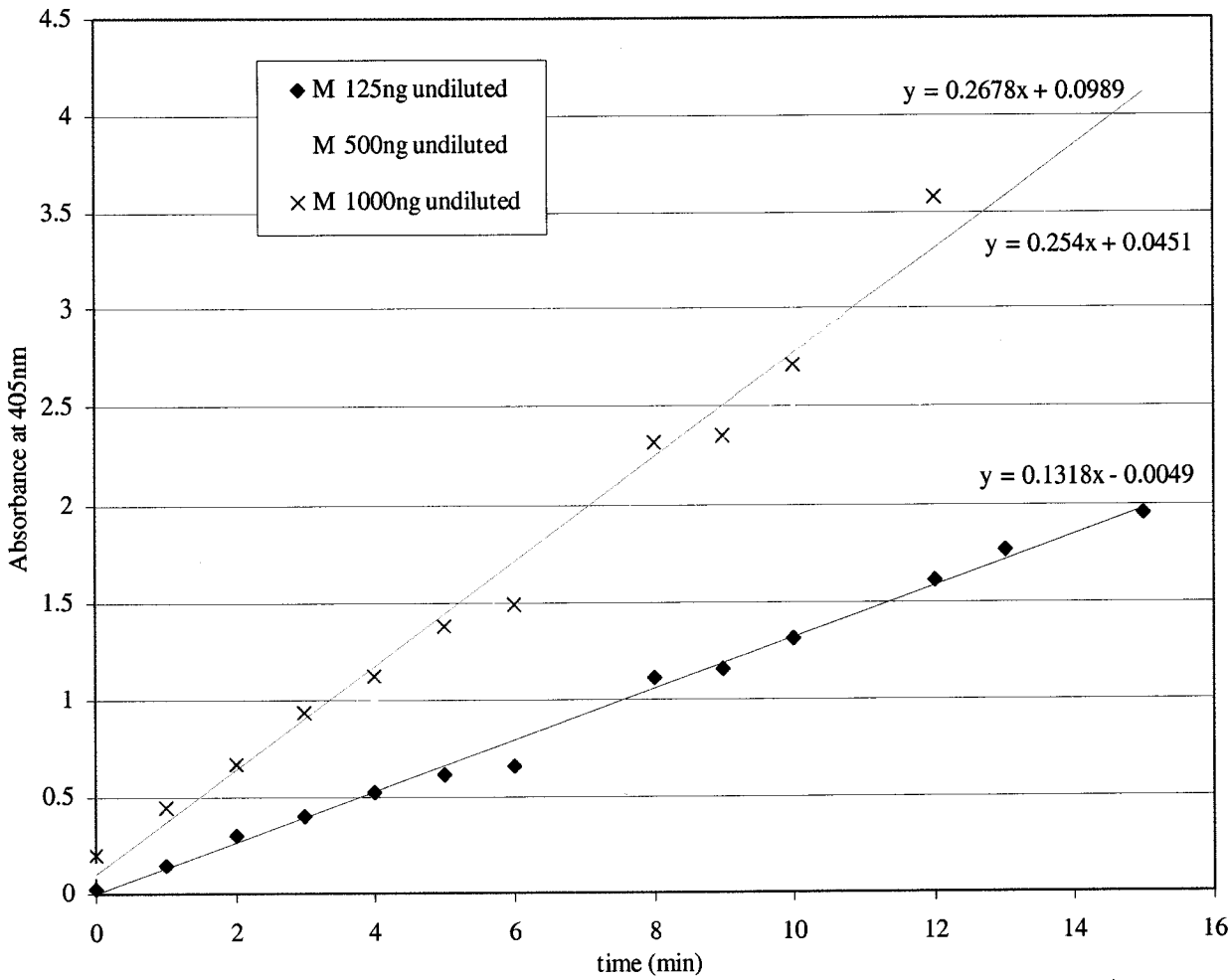
◆ M 125ng undiluted
M 500ng undiluted
× M 1000ng undiluted
y = 0.2678x + 0.0989
y = 0.254x + 0.0451
y = 0.1318x - 0.0049
Absorbance at 405nm
time (min)
0
0.5
1
1.5
2
2.5
3
3.5
4
4.5
0
2
4
6
8
10
12
14
16

Figure 7 **Optimization of the *in vitro* translation system and the CAT ELISA.** Different quantities of *in vitro* transcription mix were translated *in vitro* and then different dilutions of the *in vitro* translation mix were assayed in the CAT ELISA. The results in this figure were those of 125ng, three replicates of 250ng and 375 ng of *in vitro* transcription mix translated *in vitro*. 5 μL of these *in vitro* translations were assayed undiluted in the CAT ELISA. This graph is the absorbance at 405 nm versus time in the CAT ELISA.

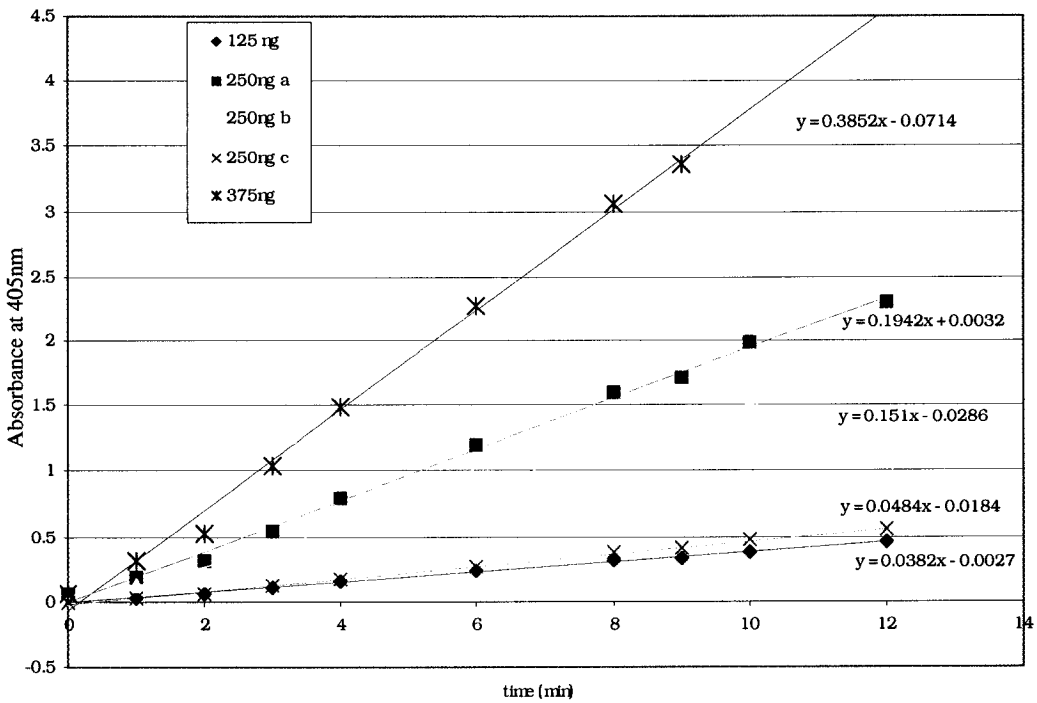
125 ng
250ng a
250ng b
250ng c
375ng
y = 0.3852x - 0.0714
y = 0.1942x + 0.0032
y = 0.151x - 0.0286
y = 0.0484x - 0.0184
y = 0.0382x - 0.0027
Absorbance at 405nm
time (min)
4.5
4
3.5
3
2.5
2
1.5
1
0.5
0
-0.5
0
2
4
6
8
10
12
14

reproducibility of the results by including a triplicate 250ng sample of the pKSCAT-M mRNA (Figure 7). From these optimization experiments, it was determined that I would use 250ng of pKSCAT mRNA as well as 50 ng of luciferase RNA in the *in vitro* translation reactions and use 5 μL of undiluted *in vitro* translation mix, in triplicate for the CAT ELISA. Prior to each experiment, all of the *in vitro* transcription reactions were analysed by agarose gel electrophoresis to determine the relative amounts of RNA by densitometry. Figure 8 is an example of a non-denaturing RNA agarose gel.

When the CAT ELISA is analysed, the absorbance at 405nm is read every minute in a plate reader. The peroxidase substrate, ABTS, yields a colour change as it is cleaved. When the results are tabulated, the absorbance over time gives a linear relationship (as seen in the preliminary data, Figures 6 and 7). The slope of this graph gives the rate of change for each pKSCAT construct that is proportional to the amount of CAT synthesized. The pKSCAT plasmids are constructs that contain one of the HPIV3 5' UTRs upstream of the CAT coding sequence. The purpose of using these constructs is to determine if the F 5' UTR decreases CAT translation compared to the other HPIV3 5' UTRs. Four experiments were carried out using two individually prepared sets of *in vitro* transcripts. Three of the experiments were carried out including luciferase RNA in the translation reaction and the fourth did not include the control RNA. There appeared to be no difference in the level of translation with and without luciferase. The rate of change results were not normalized for expression of luciferase between samples because when the data were normalized, the results for any one construct varied greatly from experiment to experiment; the unnormalized data

Figure 8 **Non-denaturing RNA electrophoresis.** The RNA samples for this gel were prepared under conditions that were RNase free. The gel as well as the running buffer were made in DEPC treated double distilled water. Lane 1: Mass Ruler mix DNA ladder (MBI Fermentas) Lane2: pKSCAT-N *in vitro* transcription mix (1 μL) Lane 3: pKSCAT-P *in vitro* transcription mix (1 μL) Lane 4: pKSCAT-C *in vitro* transcription mix (1 μL) Lane 5: pKSCAT-M *in vitro* transcription mix (1 μL) Lane 6: pKSCAT-F6 *in vitro* transcription mix (1 μL) Lane 7: pKSCAT-HN *in vitro* transcription mix (1 μL) Lane 8: pKSCAT-L *in vitro* transcription mix (1 μL).

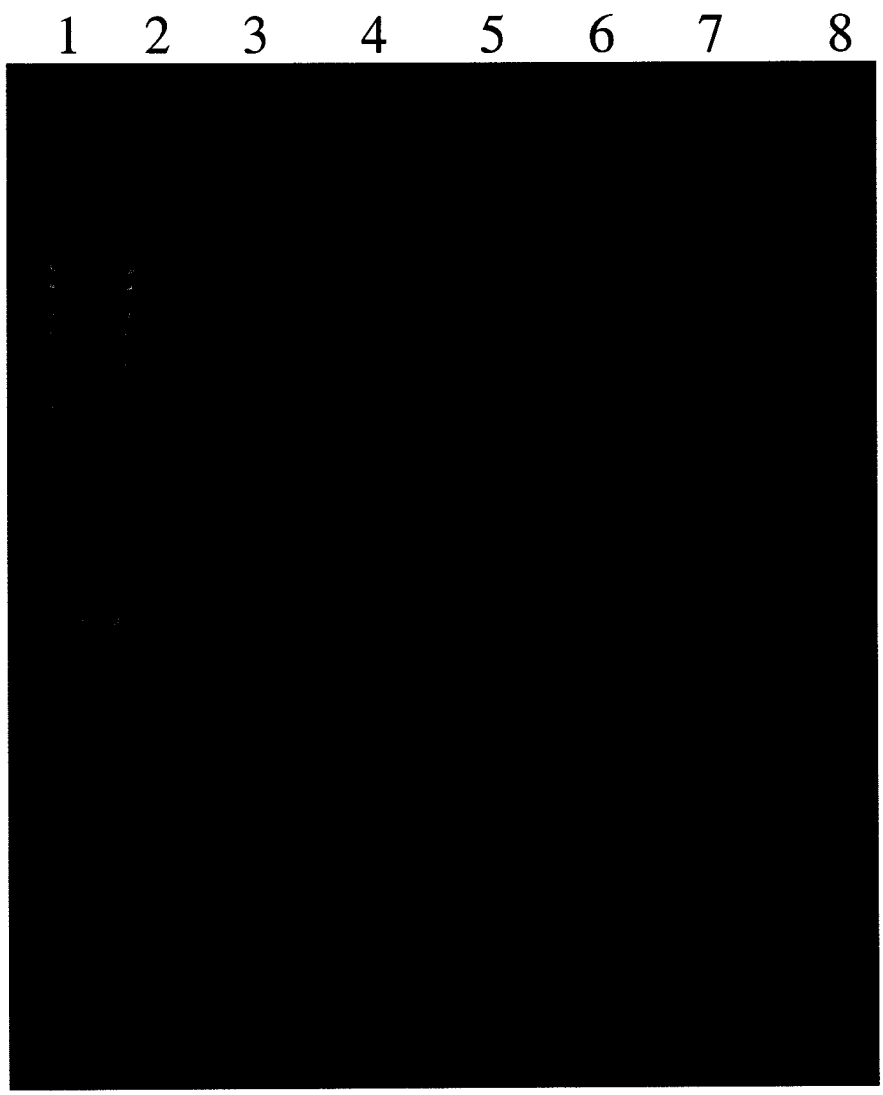
1 2 3 4 5 6 7 8

are much more consistent. For all the data, the luciferase activity of the luciferase only control was generally 2-3.6 times greater than that when the luciferase was present with CAT mRNA. This suggests that the CAT mRNA is competing with the luciferase mRNA for the translational machinery and therefore using luciferase may not be a valid control for normalizing data, because the different mRNAs may compete differently. Figure 9 shows the results from the four experiments and Figure 10 shows the average of those results. Four of the constructs gave similar results (all within the error of the other) pKSCAT-N construct had an average rate of change of 0.4 with a standard deviation of 0.03, pKSCAT-P had an average rate of change of 0.38 with a standard deviation of 0.04, pKSCAT-M had an average of 0.34 with a standard deviation of 0.04 and pKSCAT-F(6) had an average of 0.33 with a standard deviation of 0.03. Interestingly, the other three had lower average rates of change. Both pKSCAT-C and pKSCAT-L were on average approximately 2 times less active than the previous four constructs and pKSCAT-HN was approximately 11-13 times less active than the four constructs with the highest rate of change of absorbance of the ABTS substrate. pKSCAT-C had an average rate of change of 0.2 with a standard deviation of 0.08, the pKSCAT-L had an average of 0.16 with a standard deviation of 0.07 and the pKSCAT-HN had an average of 0.03 with standard deviation of 0.02.

Finally, the RNA sequences of each of the 5' UTRs were analysed using the IDT Biotools OligoAnalyzer 3.0 online. The NP 5' UTR had 6 possible hairpin structures with ΔG of -7.9 kcal/mole to -5.2 kcal/mole. The P 5' UTR had 17 possible hairpin structures with ΔG of -9.8 kcal/mole to -5.5 kcal/mole. The C 5' UTR had 19 possible hairpin

Figure 9 **The rate of change of the absorbance at 405nm for each of the pKSCAT constructs.** The data presented are for four experiments, three *in vitro* translations in the presence of luciferase RNA and one without luciferase RNA. The rate of change of the absorbance is proportional to the amount of CAT expressed in the system.

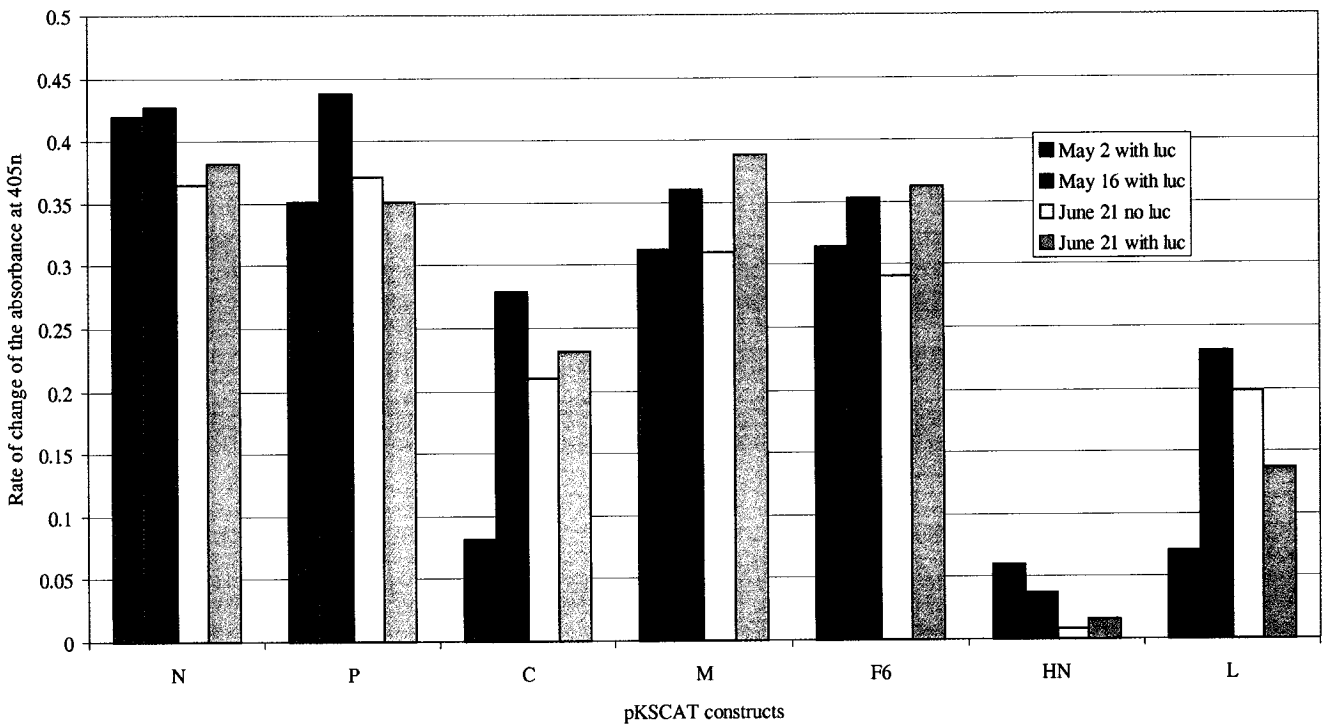
0.5
0.45
0.4
0.35
0.3
0.25
0.2
0.15
0.1
0.05
0
Rate of change of the absorbance at 405n
May 2 with luc
May 16 with luc
June 21 no luc
June 21 with luc
N
P
C
M
F6
HN
L
pKSCAT constructs

Figure 10 **The average rate of change of the absorbance at 405nm for the pKSCAT constructs.** This is the average of the four experiments seen in Figure 9. The error bars are the standard deviation of the mean.

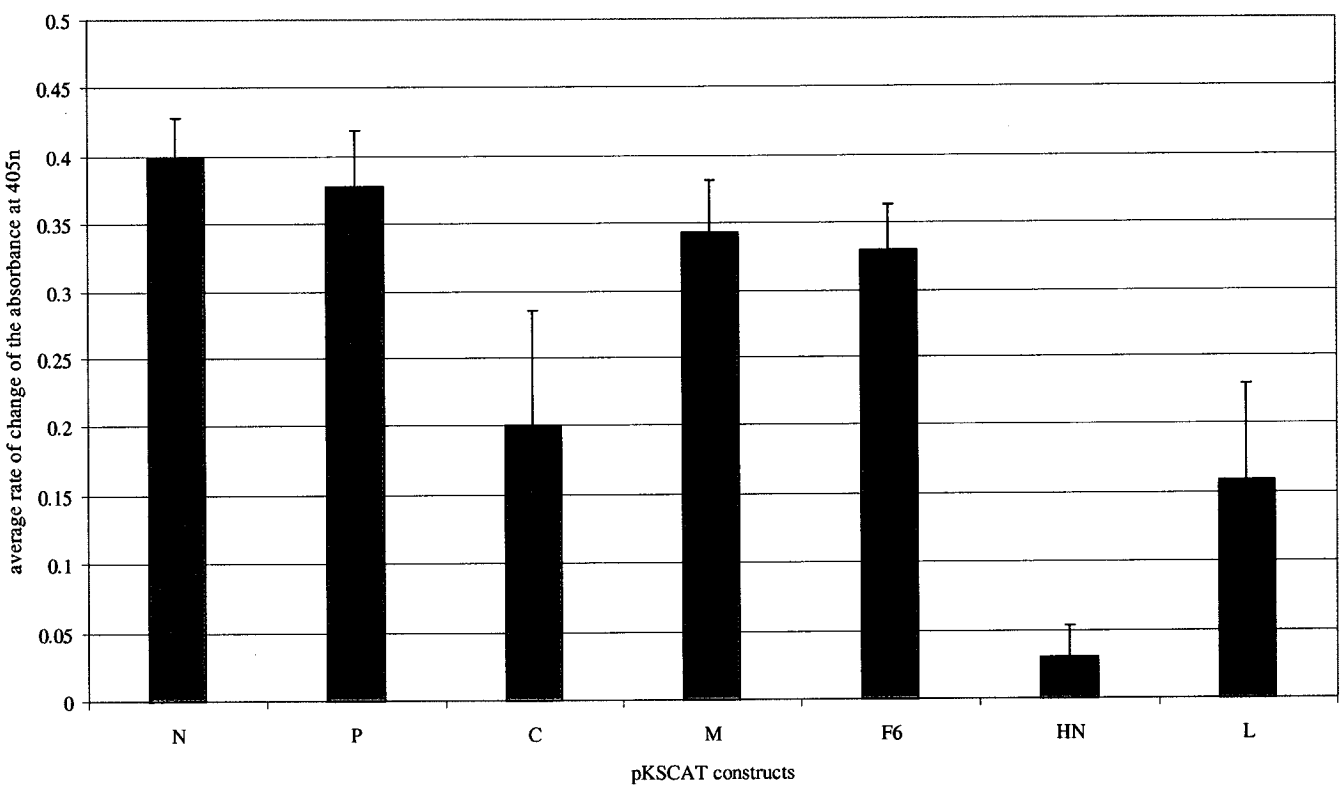
0.5
0.45
0.4
0.35
0.3
0.25
0.2
0.15
0.1
0.05
0
average rate of change of the absorbance at 405n
N
P
C
M
F6
HN
L
pKSCAT constructs

structures with ΔG of -15.3 kcal/mole to -7.8 kcal/mole. The M 5' UTR had one possible hairpin with a ΔG of 1.0 kcal/mole. The first 144 nucleotides of the F 5' UTR had twelve possible hairpin structures with ΔG of -8.1 kcal/mole to -4.03 kcal/mole. The HN 5' UTR had one possible hairpin with a ΔG of -3.9 kcal/mole and there were no possible folds for the L 5' UTR.

B. Post-Translational Regulation

In order to be active, the fusion protein must be cleaved by a protease, generally believed to be furin, in the Golgi apparatus. This cleavage releases the fusion peptide which will be exposed upon conformational changes induced by binding to the host cell receptor. Previous work in our lab has shown that as much as 50% of the fusion protein in infected cells is not cleaved (Ebata, 1996). Watanabe *et. al.* (1993) describe a set of rules that govern the cleavage of precursor proteins in all types of cells. Their rules are: " (i) The Arg at position -1 is essential. (ii) In addition to the Arg at position -1, at least two out of the three basic residues at position -2, -4, and -6 are required (the presence of all the three basic residues produces the most efficient cleavage. (iii) At position +1, a hydrophobic aliphatic residue is not suitable." The sequence of the HPIV3 cleavage site is ^{85}DPRTKR/F^{91} which adheres to most of the rules, except that there is an acidic residue at position -6. The hypothesis that is the basis for this section is that mutation of the aspartic acid at residue 85 to an arginine will create a fusion protein that is more efficiently cleaved by furin.

It was decided that this work would initially be undertaken in the context of a transient transfection system rather than a virus rescue system, for three reasons, the transfection system is faster and easier to work with, protein quantification would be easier with a tagged protein and rescue is still being developed. The Dimock lab uses the F gene of HPIV3 strain Washington 57 in a pIBI vector background for its experiments. It was decided to mutate the JS F gene in the pIBI plasmid background. The pIBIJSF construct was provided by Reza Nohkbeh. PCR based mutagenesis using two complementary mutagenic primers was carried out and mutants were screened by sequencing. None of the antibodies available in the lab could detect HPIV3 F protein on a western blot, likely because these antibodies to F are specific for conformational epitopes. Therefore, in order to visualize F and F* (the furin cleavage mutant) in a western blot it was decided to tag them with a FLAG tag because the Washington 57 strain of HPIV3 had been FLAG tagged previously and the tagged protein functions in fusion assays. The FLAG tag is a small hydrophilic octapeptide, Asp-Tyr-Lys-Asp-Asp-Asp-Asp-Lys, that is placed at the C-terminus of the HPIV3 F protein. The reason it was important to visualize the F protein and the mutant protein in a western blot was so that the extent of cleavage of each protein could be compared. This would allow me to determine by densitometry if the mutation results in more efficient cleavage of the F protein. The FLAG tagging was accomplished fairly simply by PCR amplifying the C-terminal fragment of the Washington 57 F coding sequence that included the FLAG tag and by cloning this fragment into the C-terminus of the F and F* plasmids using unique restriction sites. The C-terminal sequence of the Washington 57 strain and the JS strain are identical. All of the fusion assays and co-transfections described in this section use the

Washington 57 HN gene in pCITE-HN-flag.

Briefly, the qualitative fusion assay involves transfecting plasmids containing the F and HN sequences, under the control of the T7 promoter, into HeLaT4 cells. The cells are also infected with vTF7-3, a recombinant vaccinia virus that expresses the bacteriophage T7 RNA polymerase. The T7 RNA polymerase expressed by vTF7-3 drives the expression of the HPIV3 proteins and in the cells expressing both F and HN, fusion with neighbouring cells occurs, creating multinucleated cells, named syncytia. The cells are allowed to fuse overnight and the syncytia are analysed and counted the following morning.

In the quantitative fusion assay, a second set of cells is transfected with a plasmid containing the β-galactosidase gene, pG1N-T7βgal, however, these cells are not infected with the vaccinia virus expressing T7 RNA polymerase. Another difference is that the cells transfected with F and HN are treated with 2mU/mL of neuraminidase to temporarily prevent fusion. The neuraminidase cleaves the viral receptor sialic acid off the surface of the cells, preventing syncytium formation thus preventing the cells from fusing before the assay has been initiated (Nussbaum *et al.*, 1994). The following morning the HN + F cells are washed clean of neuraminidase and are overlayed with pG1N-T7βgal transfected cells (trypsinized after 5 hours of transfection). The theory behind this is that if the HN + F cells cause fusion, they will fuse with the β-galactosidase gene containing cells. This will cause the T7 polymerase inside the HN + F cells to begin transcribing the β-galactosidase gene and there will be expression of β-galactosidase. If no fusion occurs, then the β-galactosidase will not

be expressed. The cells are then lysed and the lysates are mixed with CPRG, a substrate of β-galactosidase, the amount of β-galactosidase present in the cells (as detected by spectrophotometry) is a direct measurement of the amount of fusion occurring in the HN + F well.

Tables 3a and 3b give the results of a qualitative fusion assay comparing syncytium formation induced following transfection of HeLaT4 cells with pIBIJSF-flag or pIBIJSF*-flag and pCITEHN-flag at different pIBIJSF (F*) to pCITEHN ratios. The same plasmid ratios were also used for the quantitative fusion assay. Because from experiment to experiment there were slight variations in the confluency of the cells or the stage of the cellular cycle that the cells are in, the experiments cannot be averaged together. However, there is a general trend that establishes itself from fusion assay to fusion assay. There is increased fusion with F* and this is confirmed in the quantitative assay.

The experiment with ratios of F or F* to HN DNA ranging from 1:80 to 1:2.5 were carried out twice in duplicate and the experiment with ratios of F or F* to HN DNA ranging from 1:1000 or 1:200 to 1:1 were carried out three times in duplicate. To confirm the concentration of DNA, the pIBIJSF, pIBIJSF* and pCITEHN plasmids were linearized and analysed by agarose gel electrophoresis and their concentration determined by densitometry against a ladder of known concentration. The fusion index is the rate of production of β-galactosidase relative to time, determined using CPRG as a substrate. The fusion index bears a direct relationship to the amount of fusion that occurred in each well. One trend observed

Table 3A Qualitative fusion assay following transfection of cells with F and HN plasmids

Plasmid (with FLAG tag)	ratio of F to HN DNA	relative amount of syncytia	Plasmid (with FLAG tag)	ratio of F* to HN DNA	relative amount of syncytia
pCITEHN only	n/a	n/a			
pIBIJSF* only	n/a	n/a			
pIBIJSF only	n/a	n/a			
pIBIJSF	1:80	(++++)	pIBIJSF*	1:80	(++++)
pIBIJSF	1:40	(+++)	pIBIJSF*	1:40	(++++)
pIBIJSF	1:20	(+++)	pIBIJSF*	1:20	(++++)
pIBIJSF	1:10	(+ ½)	pIBIJSF*	1:10	(++)
pIBIJSF	1:5	(+)	pIBIJSF*	1:5	(++)
pIBIJSF	1:2.5	(½)	pIBIJSF*	1:2.5	(+)

Table 3B Qualitative fusion assay following transfection of cells with F and HN plasmids

Plasmid (with FLAG tag)	ratio of F to HN DNA	relative amount of syncytia	Plasmid (with FLAG tag)	ratio of F* to HN DNA	relative amount of syncytia
pCITEHN only	n/a	n/a			
pIBIJSF* only	n/a	n/a			
pIBIJSF only	n/a	n/a			
pIBIJSF	1:1000	(½)	pIBIJSF*	1:1000	(½)
pIBIJSF	1:100	(+++)	pIBIJSF*	1:100	(++)
pIBIJSF	1:10	(++)	pIBIJSF*	1:10	(+++)
pIBIJSF	1:1	(+)	pIBIJSF*	1:1	(+)

Legend: ++++ indicates 70-90% syncytia per field
+++ indicates 50-70% syncytia per field
++ indicates 30-50% syncytia per field
+ indicates 20-30% syncytia per field
½ indicates less than 20% syncytia per field

in all the quantitative fusion assays is that as the ratio of F to HN decreases, that is, as the amount of F in the system increases, the amount of fusion observed decreases. Another trend is that the amount of fusion observed in the wells with F* is consistently higher than that observed for the wild type F at almost every ratio (Figures 11a and 11b). The only point not shown, is the 1:1000 ratio, (it was only carried out twice), the value (for one experiment) of the normalized fusion index for F is 0.24 and for F* 0.31. This is the only ratio where the values for F and F* are similar.

One explanation for the observations was that the mutant F was cleaved to a greater extent than the wild type F. To test this possibility, both F genes were expressed in the presence and absence of the HN gene in HeLaT4 cells. The cells were lysed and the proteins were analysed by SDS-PAGE and Western blotting, using an anti-FLAG antibody. The relative amounts of F_0 and F_1 present in each sample were determined by densitometry and the percent cleavage was calculated. These calculations were based on densitometry of the Western blot film, the background was removed and the ratio of cleaved protein (F_1) over total protein $F_1 + F_0$ was calculated.

F-flag and F*-flag were cleaved to approximately the same degree in the absence of HN, 16.9% ± 9 and 18% ± 6.8 cleavage respectively (this value is an average from 6 Western blots). The Western blots also show that the cleavage of both F and F* is enhanced in the presence of HN. Cleavage in the presence of HN was typically 2.2-2.6 times more cleavage than without HN. The average percent cleavage of the mutant protein in the presence of HN

Figure 11 **Quantitative fusion assay.** Normalized fusion index versus ratio of F to HN DNA. The HeLA T4 cells were transfected with various ratios of F or F* to HN DNA in 24 well dishes. These cells were treated with 2 mU/mL of *Vibrio cholerae* neuraminidase prior to overnight incubation. The F and HN cells were overlayed with cells transfected with pG1N-T7βgal. The cells were lysed and the lysate mixed with CPRG. The absorbance at 540nm was plotted over time. The slope of that graph gives the fusion index, which is proportional to the amount of fusion that occurred in each well. **A)** One experiment with ratios of F to HN between 1:80 and 1:2.5. **B)** A separate experiment carried out in parallel with ratios of F to HN between 1:1 and 1:200.

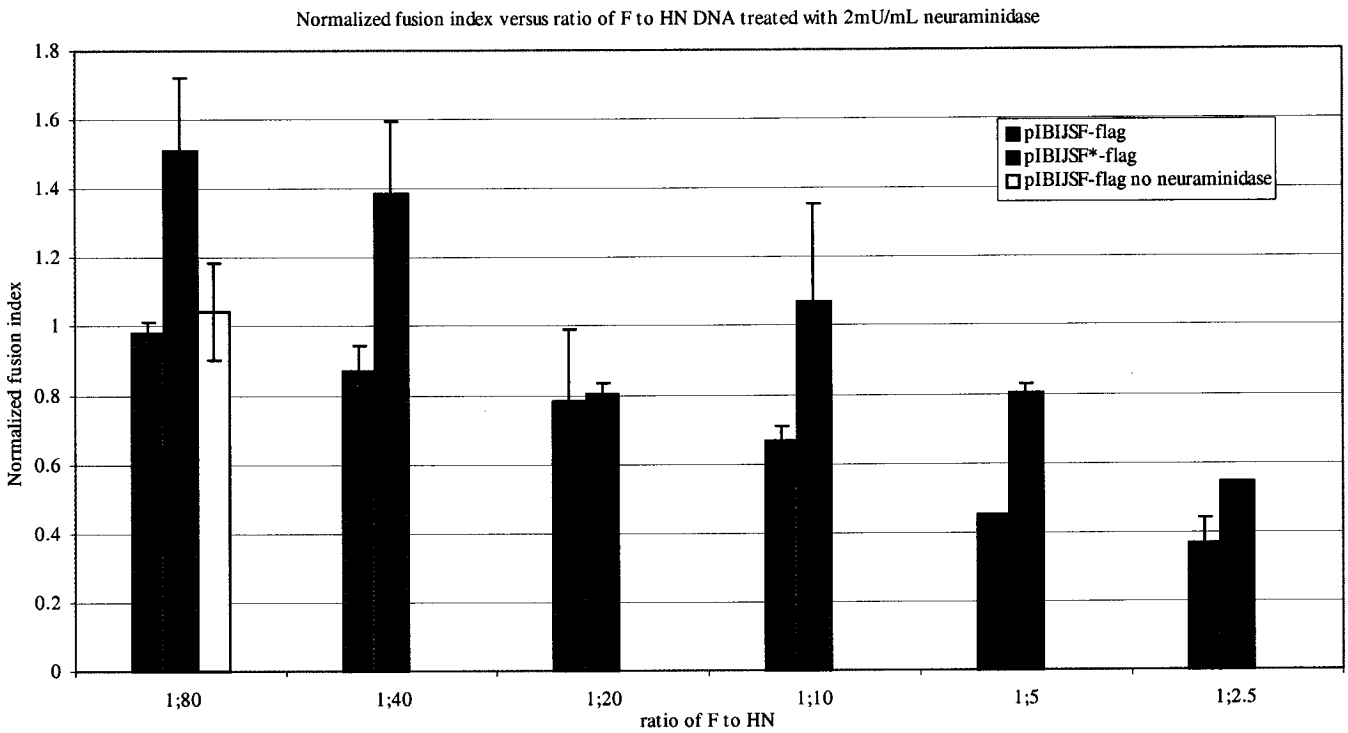
Normalized fusion index versus ratio of F to HN DNA treated with 2mU/mL neuraminidase
Normalized fusion index
1.8
1.6
1.4
1.2
1
0.8
0.6
0.4
0.2
0
pIBIJSF-flag
pIBIJSF*-flag
pIBIJSF-flag no neuraminidase
1;80
1;40
1;20
1;10
1;5
1;2.5
ratio of F to HN

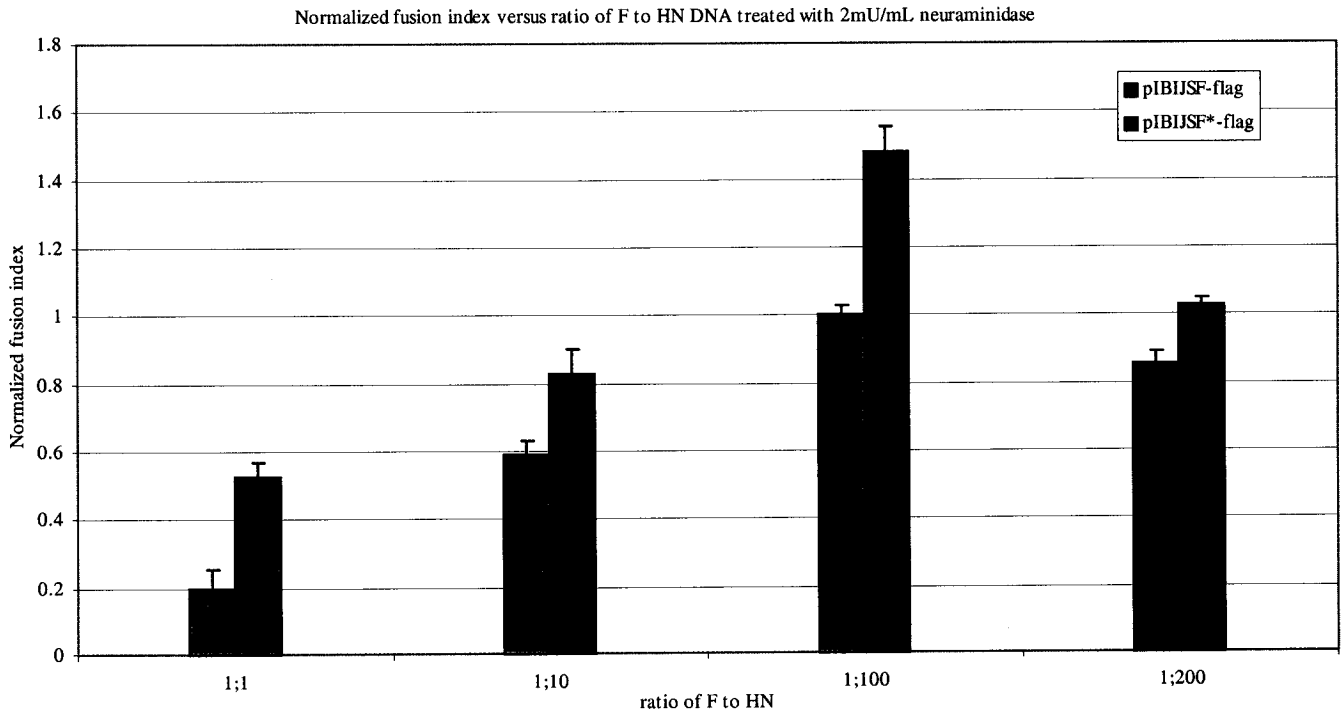
Normalized fusion index versus ratio of F to HN DNA treated with 2mU/mL neuraminidase
Normalized fusion index
1.8
1.6
1.4
1.2
1
0.8
0.6
0.4
0.2
0
pIBIJSF-flag
pIBIJSF*-flag
1;1
1;10
1;100
1;200
ratio of F to HN

was 48.38% with a standard deviation of 7.2, whereas that of the wild-type was on average 34.16% with a standard deviation of 10.6. There is a fair amount of variation from Western Blot to Western Blot in the ratio of cleavage, likely due to variations in cell density on transfection but also due to background on the film that causes difficulty with the densitometry. Nevertheless, sometimes there is as much as 2.5 times more cleavage with the mutant F in the presence of HN than the wild-type. Although the errors seem large, for each Western blot, there is a noticeable difference in the extent of cleavage of F or F* in the presence or absence of HN. Figure 12a is a representative Western Blot and Figure 12b is the densitometry data for Figure 12a.

Figure 12 **Western Blot and quantification of F protein cleavage. A)** Western Blot (9% SDS-PAGE, with a 5% stacking gel) of cell lysates transfected with pIBIJSF-flag or pIBIJSF*-flag in the presence and absence of pCITEHN-flag. The mock cells were transfected with pCR2.1Topo plasmid DNA. The primary antibody was mouse anti-FLAG M2 (1:10 000) and the secondary antibody was rabbit anti-mouse IgG conjugated with horseradish peroxidase. The chemiluminescence signal was developped with luminol, p-cumeric acid and H_2O_2, and was exposed to film. Lane 1: JSF-flag without HN-flag, lane 2: JSF*-flag without HN-flag, lane 3: JSF-flag with HN-flag, lane 4: JSF*-flag with HN-flag, lane 5: Mock transfected. **B)** The bands corresponding to F_0 and F_1 were analysed by densitometry and the film background was removed (the values are integrated density values as generated by the AlphaEase™ software version 3.3b_gc (Alpha Innotech Corporation)).

A)

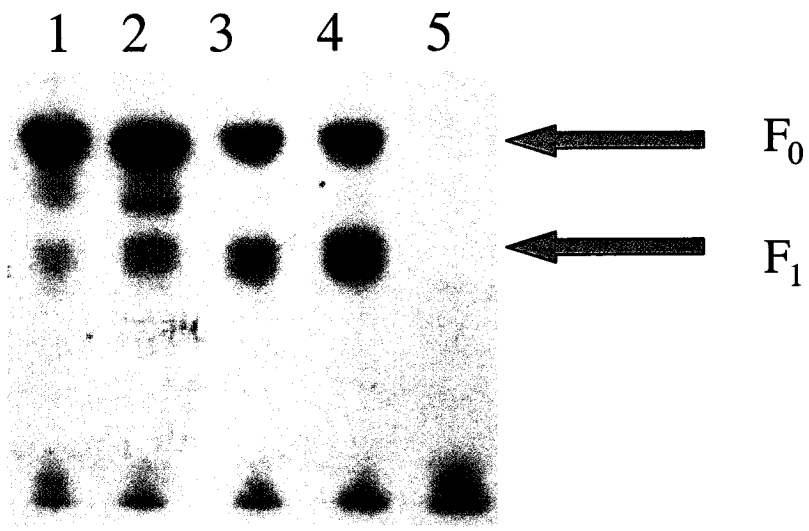

B)

	without HN		with HN	
	F-flag	F*-flag	F-flag	F*-flag
F0	73008 [1]	85175	38376	45864
F1	13104	23400	23400	55224
% cleavage	15.22 % [2]	21.55 %	37.88 %	54.63 %

[1] integrated density value with the film background subtracted from each value
[2] % cleavage=F_1/F_1+F_0 x 100

C) Preparation of plasmids for rescue of HPIV3

The next phase in the study of the regulation of HPIV3 fusion protein expression is to study mutant F or the transcriptional readthrough of the M-F gene junction in a biologically relevant model; viruses that express mutations. This would be accomplished using a reverse genetics virus rescue of HPIV3. In preparation for the eventual rescue of the virus, a number of key constructs needed to be prepared. This final results section deals with the preparation of the plasmid constructs for HPIV3 rescue.

Preliminary experiments were undertaken to ensure that the three support plasmids expressing the NP, P without the C ORF and the L proteins; pTM(N), pTM(PnoC) and pTM(L) respectively, were functional. This was accomplished using the mini-genome rescue system with a synthetic HPIV3 mini-genome containing the luciferase ORF (Jogalakar, 2000). The plasmids were functional in the mini-genome system. Various preparations of MVA-T7 were assayed for T7 RNA polymerase expression, using the β-galactosidase assay with cells transfected with pβGalT7 plasmid. Most preparations of MVA-T7 expressed β-galactosidase, however the amounts expressed varied. Rescue of HPIV3 from p2G was attempted seven times, using various preparations of MVA-T7. The supernatant from the rescue after 2 passes in LLC-MK2 cells was negative for HPIV3. This work was put on hold, because the rescue of HPIV3 was repeatedly unsuccessful and my efforts were redirected to the previous two projects.

IV. DISCUSSION

The paramyxovirus fusion protein is a key regulator of virulence (Peeters *et al.*, 1999). In its cleaved form, it is essential for virus infectivity, however it does not need to be fusion active (ie. cleaved) to be packaged into virions (Watanabe *et al.*, 1995). It has been observed, in transfection studies on HPIV3 as well as HPIV1, that expression of high amounts of F cause a downregulation in the amount of HN expressed (McKenna, unpublished data and Bousse *et al.*, 1997). This suggests that regulation of F protein expression in HPIV3 infected cells is essential to prevent downregulation of other viral proteins, such as HN, and to allow infection to proceed. When this work was initiated, I hypothesized that the expression of functional HPIV3 F protein was regulated by three possible mechanisms: 1) transcriptional regulation at the M/F gene junction, 2) translational regulation of F expression by the long 5' UTR and 3) F protein processing.

Previous work in the Dimock lab has shown that the 8 extra nucleotides present at the M/F gene junction are necessary and sufficient to cause approximately 88% transcriptional read-through (Jogalakar, 2000). This causes an immediate decrease in the amount of F mRNA that can be translated into F protein. Transcriptional regulation is a key regulatory mechanism for many viruses (Conzelmann, 1998). One experiment that is planned is to create a recombinant HPIV3 virus in which the 8 extra nucleotides at the M/F gene junction have been removed. Based on the results from the mini-genome studies, this would arrest transcriptional read-through and therefore increase the amount of F mRNA that

can be translated. Our lab is very interested in the affect this will have on the virus, in terms of virulence, replication, or on the expression of the downstream genes, HN and L.

A. Translational Regulation:

My initial hypothesis regarding the translational regulation of the F mRNA was that the long 5' UTR would diminish the efficiency of translation of the downstream open reading frame. This hypothesis was based on the fact that certain 5' UTRs are inhibitory to translation of the downstream ORF, for example the 5' UTR of the transforming growth factor beta (TGF-β) gene.

The 5' UTRs of all the HPIV3 mRNAs were placed upstream of the CAT ORF in various plasmid constructs. The amount of CAT synthesized following *in vitro* transcription and translation was determined. Synthesis of CAT was similar when the 5'UTRs of the HPIV3 F, NP, P and M mRNAs were located upstream of the CAT ORF. However, the C, HN, and L 5' UTRs all had inhibitory effects on CAT synthesis. The 5' UTR of the C and L genes inhibited CAT synthesis two-fold and the 5' UTR of the HN gene inhibited CAT expression more than ten-fold, as compared to the other four 5'UTRs.

Luciferase mRNA was added to the *in vitro* translation mixtures so that CAT expression could be normalized relative to luciferase expression. When the data were analysed, it was noted that luciferase expression varied considerably from sample to sample

and this led to large deviations that confounded the data. The luciferase only control also expressed much more luciferase than did the samples with CAT mRNA, therefore most likely, the two mRNAs were competing, rendering the luciferase normalization invalid. There was, however, no noticeable difference in CAT expression in the presence and absence of luciferase.

As previously discussed, Davuluri *et. al.* have devised a computational classification of mRNAs based on analysis of their 5' UTR sequences. Class I mRNAs encode inefficiently translated proteins such as transcription factors and regulatory proteins (Davuluri *et. al.* 2000). Class II mRNAs have a (5') terminal oligopyrimidine tract (TOP) and are regulated in a growth dependent fashion (Davuluri *et. al.* 2000). A TOP is a stretch of 4-14 pyrimidines that always starts with a C at the cap site (Meyuhas, 2000). Another characteristic of mRNAs that contain a TOP is that it is followed by a CG rich region and the 5' UTR is devoid of upstream AUGs (uAUGs) (Meyuhas, 2000). Translation of TOP-containing mRNAs is thought to be repressed by a pyrimidine binding protein (Meyuhas, 2000). Finally, class III genes are highly expressed, transcriptionally regulated and, most likely, efficiently translated (Davuluri *et. al.* 2000). In fact, Davuluri *et. al.* (2000) have determined that the most discriminating variables among the three classes of mRNAs are the presence of a TOP, the 5' UTR length, the presence of a stable secondary structure within the first 100 bases from the cap site, the A/T and G/C ratios, the number of upstream AUGs (uAUGs) and the number of upstream ORFs (uORFs).

Interestingly, 95% of the mRNAs in class I (the poorly translated proteins) had 5' UTRs longer than 100 bases, whereas the average length of 5' UTRs for class II mRNAs was 45 and for those in class III 73 nucleotides (Davuluri *et. al.* 2000). Keeping with this trend, over 90% of the class I transcripts have stable secondary structures with average free energies less than -50 kcal/mol, while mRNAs from classes II and III are nearly devoid of this feature (Davuluri *et. al.* 2000). Kozak (1991) reviewed the rules with regard to secondary structure between the cap and the AUG. Secondary structure in this region never facilitates translation initiation; it may have little effect or it may impair initiation (Kozak, 1991). Secondary structure within the first 12 nucleotides of the cap inhibits translation (Kozak, 1991). Also, if the AUG is within the first 12 nucleotides of the cap, initiation is impaired (Kozak, 1991). Between the cap and the AUG, it is the stability of any secondary structure that determines its effect on translation; a stem-loop structure with a free energy of -30 kcal/mol does not impair translation, whereas a similar structure with -50 to - 60 kcal/mol free energy inhibits translation to a very great degree (Kozak, 1991). There are no known mechanisms for modulating the inhibitory effects of secondary structure (Kozak, 2002).

Davuluri *et. al.* demonstrated that 65 % of the transcripts in class II have AUGs in good context, class III have 57% and class I have 49% of AUGs in good context for initiation (Davuluri *et. al.* 2000).

With regards to the uAUGs, 42% of class I mRNAs have uAUGs and 32% have uORFs whereas uAUGs were absent in class II mRNAs and three times less frequent in class

III mRNAs (Davuluri *et. al.* 2000). Lending weight to these findings are other studies that have found uAUGs in nearly two-thirds of oncogenes as well as in genes that control cellular growth and differentiation (Morris and Geballe, 2000). If the uAUG encodes an uORF (ie. if there is a stop codon before the AUG for the major gene product) then the 40S subunit remains bound to the mRNA and can scan and reinitiate translation downstream (Kozak, 2002; Morris and Geballe, 2000). There are a number of factors that control this mechanism. The first is the length of the uORF. This is thought to be the case because certain necessary translation factors (as yet uncharacterized) dissociate from the ribosome gradually and, if the uORF is sufficiently short, these factors remain bound to the ribosome (Kozak, 2002). The permissible length most likely varies depending on the mRNA, however, reinitiation has been observed after translation of a 12 codon uORF, but was abolished after a 33 codon uORF (Kozak, 2002). The intercistronic sequence must also be sufficiently long to allow the 40S subunit to reacquire the Met-$tRNA_i$, a necessary step for reinitiation (Kozak, 2002). An intercistronic space that is 50-80 nucleotides or longer diminishes or removes any inhibitory effect of the uORF (Morris and Geballe, 2000). In certain cases it is not only the length of the intercistronic region that determines its effect, but also its sequence.

Not a single one of the HPIV3 mRNAs contains the optimal Kozak consensus sequence, GCCA/GCC$\underline{a^{+1}ug}$G surrounding the AUG. However, all, except for the P 5' UTR, have an A or a G at the -3 position, and, for these experiments, all have a G at the +4 position (this is part of the CAT gene sequence). In nature, the nucleotide at the +4 position of the NP gene is a U, for the P, HN, and L genes position +4 is a G, for the C and F genes

it is a C, and for the M gene it is an A.

Analysis of the three 5' UTRs that lowered translation of CAT (from the C, L and HN genes) points to some overlooked but obvious characteristics that could explain these observations. The easiest to explain is the 5' UTR of the C mRNA. This 5' UTR is identical to that of the P mRNA except that it includes and extends 7 nucleotides past the AUG for the P protein. The obvious characteristic of this 5' UTR is that it contains the AUG for the P protein, thus creating an mRNA with an uAUG out of frame with the CAT coding sequence, at which translation could be initiated and decreasing the amount of CAT expressed. There is some evidence that the sendai virus C protein causes apoptosis in infected cells (Itoh *et al.*, 1998). The amount of C protein that causes some cytopathic effect in the cells but not so much that the virus life cycle is cut short, may be critical. My data suggest that there may be an element of translational downregulation of C expression by the C 5' UTR which may play a role in the regulation of virus propagation.

The 5' UTR of the L mRNA is the shortest of all the HPIV3 5' UTRs, at 12 nucleotides. Closer examination of the L mRNA 5' UTR reveals an uAUG at the second nucleotide. This AUG is not in a good context for translation initiation, however, if it is used, it may decrease the efficiency with which the L protein AUG is utilized. Also, the A of the L AUG is the 13th nucleotide, which is likely too close to the cap for efficient initiation, causing a downregulation in the expression of the gene (or the reporter) (Kozak, 1991).

An explanation for reduced CAT expression when the HN 5' UTR is upstream of the CAT ORF is more obscure than for the C and L 5' UTRs. There does not appear to be any major secondary structure in the 63 nucleotide 5' UTR, the one possible hairpin structure has a free energy of -3.9 kcal/mole, far below the -50 kcal/mol that can obstruct scanning of the mRNA by the 40S ribosomal subunit (Kowalski and Mager, 1998). There are no uAUGs. There is no terminal oligopyrimidine tract. The AUG, while not in the consensus Kozak sequence, has a G at position -3 which should indicate a good context for ribosomal initiation. There may simply be an element of the sequence of the 5' UTR that is not conducive to high expression of the downstream gene.

Generally, a 5'-UTR that directs efficient translation is short, has low G-C content (no secondary structure) and does not contain upstream AUGs (Meijer and Thomas, 2002). Interestingly, Kozak cites certain long linear 5' UTRs as increasing translation of the mRNA (Kozak, 1991). There is a requirement for approximately 20 nucleotides after the cap for the initiation of the 40S subunit to occur properly (Kozak, 1991). It has been shown that the addition of long synthetic 5'-UTR to expression vector genes is a simple way to increase translational efficiency (Kozak, 1991).

The efficient translation of an mRNA containing long linear 5' UTRs may be what is occurring with the long 5' UTR of the F mRNA. The 5' UTR, which is very A rich, seems to be free of hairpin structures and may simply be a way of ensuring good translation of the F mRNA, especially if the amount of F mRNA is drastically downregulated by read-though

transcription.

The next step in this investigation would be to transcribe all the pKSCAT plasmids with a cap. This would allow analysis of the effect of the cap; does it increase the relative levels of translation? Do the trends seen with uncapped mRNA hold true for a capped mRNA? *In vivo*, the HPIV3 mRNAs are all capped in the cytoplasm of the infected cell, therefore capping the transcripts may be more biologically relevant. Another set of experiments would be to perform site-directed mutagenesis of certain key elements of the 5' UTR of the C, HN and L mRNAs. For example, for the C 5' UTR, it would be very interesting to determine if the removal of the uAUG would increase translational efficiency. For the L 5' UTR, it would be interesting to remove the uAUG and see what happens. Also for the L 5' UTR, it would be interesting to gradually increase the length of the 5' UTR to see what effect it has on translation. Another set of experiments could be planned that determine the effect of other viral components on the efficiency of translation. This would involve transfecting the capped or even the uncapped mRNA into HPIV3-infected or uninfected cells and determine the amount of CAT expression. Similar experiments have been done in the coronavirus system. (Senanayake and Brian, 1999). Approximately half as much CAT was expressed, both *in vitro* and in uninfected cells when the 210 nucleotide 5' UTR for coronavirus mRNA 1 was upstream of the CAT ORF, by comparison with the 77 nucleotide mRNA 7 5' UTR (Senanayake and Brian, 1999). However, they observed a 12 fold decrease when the same transcripts were translated in coronavirus infected cells (Senanayake and Brian, 1999). It would be interesting to know if viral or virally induced cellular trans-

activating factors exist in HPIV3 infected cells (Senanayake and Brian, 1999).

My initial hypothesis was that translation of CAT with the F 5' UTR would be less efficient than with other 5'UTR's. I found the opposite effect. Increased translation due to the F gene 5' UTR may have evolved to compensate for transcriptional downregulation of F mRNA synthesis. It is also possible that the read-through transcription at the M/F gene junction ensures that sufficient amounts of HN and/or or L are synthesized (Parks *et al.*, 2001). Parks *et al.* created a recombinant SV5 mutant with increased read-through at the M/F gene junction; this caused a global decrease in viral mRNA and protein synthesis (Parks *et al.*, 2001). They hypothesize that the read-through transcription at the SV5 M/F gene junction is a means of fine-tuning the amount of polymerase expressed (Parks *et al.*, 2001). I suggest that translational controls in the form of the 5' UTR is also a mechanism for fine-tuning the levels of all three proteins downstream of the M/F junction, to enhance F, and to decrease HN and L. The reasoning behind this model is that readthrough at the M/F junction increases the amount of viral polymerases that can transcribe the HN and L genes (because there are fewer polymerase molecules that fail to reinitiate at the F start sequence), therefore, the amounts of HN and L synthesized must also be regulated translationally. The results of this research suggest that it would be of considerable interest to follow up on the regulation of HPIV3 mRNA translation.

B. Proteolytic processing as a means of regulation

My initial hypothesis with regards to the proteolytic processing of F was that the sequence of the HPIV3 F protein ensures that cleavage of F is less than 100% efficient. My original goal regarding this section of my research was to determine if changing the furin cleavage site in F from ^{85}DPRTKR/F^{91} to ^{85}RPRTKR/F^{91} would cause the fusion protein to be more efficiently cleaved. I also wanted to determine the effect of this change on syncytium formation.

Watanabe *et al.* (1993) describes the following rules with regards to furin cleavage: i) an Arg at position -1 relative to the cleavage site is indispensable; ii) in addition to the Arg at position -1, at least two of the three positions: -2, -4 and -6 must have a basic amino acid for efficient cleavage (if all three residues are basic, the result is the most efficient cleavage); iii) a hydrophobic aliphatic amino acid at position +1 is not desirable (Watanabe *et al.*, 1993).

The first results obtained from the qualitative fusion assay (Table 3a and 3b) demonstrated that the F protein containing the modified cleavage site, F*, was active, and caused HeLaT4 cells in culture to fuse when co-expressed with HPIV3 HN. Expression of individual flag-tagged F, F* or HN did not cause syncytium formation nor were they toxic to the cells. Generally, F*-flag DNA, when transfected into cells with pCITEHN-flag cause slightly more fusion than F-flag with the same ratio of HN. For this assay, the maximum

amount of fusion for F-flag occurred at a ratio of F to HN DNA of approximately 1:80. The maximum for F*-flag occurred at a ratio of F to HN DNA of approximately 1:40-1:80. At the lowest F to HN DNA ratio (1:1000), there was very little fusion with F-flag or F*-flag. Presumably, insufficient quantities of the F protein are synthesized to cause fusion. Reduced fusion was also observed at high F to HN DNA ratios (1:1). This may be related to what is observed in Western blots when F and HN are co-expressed in cells. When HN is expressed by itself a visible band is readily detected on Western blots (McKenna, unpublished data). When F and HN-encoding plasmids are transfected into cells at a 1:10 ratio, a band for the F protein is clearly visible, however the band for HN is faint or absent (McKenna, unpublished data). This can also be seen in Figure 12, the band for HN-flag should be just above the F_0 band, however it is absent. Tanaka *et al.* (1996) have also observed this phenomenon, HPIV3 F protein downregulating HN protein expression. They suggest that this is a mechanism for regulating syncytium formation. This phenomenon was what inspired the idea that F protein expression must be tightly regulated, because if F is over-expressed, then HN is repressed. This would likely affect HPIV3 replication as well as syncytium formation because of the small amounts of HN glycoprotein that would be available for assembly if F expression was not regulated.

The results obtained with the qualitative fusion assay were confirmed with the quantitative assay. Maximum fusion occurred at F to HN DNA ratios of 1:40, 1:80 and 1:100. F*-flag consistently caused more fusion than F-flag at every F to HN DNA ratio, except ratios of 1:20 and 1:1000. The variability observed at 1:20 is an outlier due to

experimental error. The small differences seen at the 1:1000 F to HN DNA ratio is likely due to the low level of fusion. On average, the fusion index of F*-flag is approximately 1.5 times greater than that of F-flag (if one ignores error and the data for the 1:20 F to HN ratio).

The bell shaped graph (Figure 11b) is interesting, because it is counter-intuitive. Intuitively, if the quantity of F DNA is increased and the quantity of HN DNA remains the same, then the amount of fusion should increase, not decrease as seen in Figure 11b. This may be related to the evidence that the F and HN proteins interact (McGinnes *et al.*, 2002; McKenna, unpublished; Stone-Hulslander and Morrison, 1997; Tanaka, *et al.*, 1996) most likely in the endoplasmic reticulum (ER) as shown in a study that added an ER localization signal (KDEL) to F and observed a certain amount of retention of HN in the ER (Tanaka, *et al.*, 1996; Tong and Compans, 1999). In a transfection system, the HPIV1 F protein also appears to downregulate HN expression as compared to infected cells (Bousse *et al.*, 1997). Because HN mRNA levels were unaffected, this downregulation is believed to be a post-transcriptional event. The amount of HPIV1 HN protein in infected cells is greater than the amount of HPIV1 F protein, suggesting that F protein synthesis is regulated and downregulation of HN does not occur. Accordingly, the fusion results in Figure 11b indicate that there is an optimal F to HN ratio for fusion. Insufficient F protein results in less fusion. Excess F protein, which has the effect of lowering the amount of HN protein, also results in less fusion.

The fusion assays suggested that F*-flag was more fusogenic than F-flag. However,

it was necessary to determine if similar amounts of the two proteins were being expressed in transfected cells and if the extent of cleavage was similar for F*-flag and F-flag. Western blot analysis (Figure 12) was performed on lysates of cells expressing F*flag or F-flag in the presence or absence of HN and showed that cleavage of both F*-flag and F-flag were enhanced more than two-fold in the presence of HN. Also, F*-flag was cleaved 1.4 times more efficiently than F-flag in the presence of HN.

Together, the fusion assay data and the Western analysis, are consistent with the interpretation that mutation of the cleavage site from ^{85}DPRTKRF^{91} to ^{85}RPRTKRF^{91} increases susceptibility of the HPIV3 F protein to furin cleavage in the presence of HPIV3 HN. Why is the cleavage of the F protein enhanced in the presence of HN? My hypothesis is that F and HN interact together in either the ER or the cis-Golgi network, before reaching the trans-Golgi, where furin accumulates (Tanaka *et al.*, 1996). Due to this interaction, the furin cleavage site in F_0 is more exposed and more accessible to furin, therefore cleavage is enhanced in the presence of HN. Trudy Morrison's group has evidence that lends weight to my hypothesis. They have demonstrated that an antibody to heptad repeat 1 (HR1) of the NDV F protein binds to uncleaved, cell surface F protein, in a manner that is dependant on co-expression of NDV HN (McGinnes *et al.*, 2002). Therefore, interaction of NDV HN with F_0 exposes an antigenic site that contains HR1; HR1 is near the cleavage site, this is consistent with the possibility that HN interaction with F_0 facilitates cleavage.

C. Preparation of plasmids and virus stocks for rescue of HPIV3

In preparation for HPIV3 rescue from cDNA, certain plasmids and virus stocks needed to be prepared. The full length HPIV3 JS strain genomic plasmid p2G has been modified by including a unique Sbf I site at position 4372. This will allow modification of the sequences at the end of the M gene and the beginning of the F gene. Two constructs have been made and simply need to be cloned into the p2G-sbf, one of these constructs incorporates the deletion of the 8 extra nucleotides at the M /F gene junction and the other incorporates a unique BstZ17I site at the end of the L gene. MVA-T7 has been grown to fairly high titre in BHK cells and expresses T7 RNA polymerase. All of these tool will be useful once rescue is up and running in our lab.

REFERENCES

Band, A., J. Määttä, L. Kääriäinen, and E. Kuismanen. 2001. Inhibition of the membrane fusion machinery prevents exit from the TGN and proteolytic processing by furin. FEBS Let. 505:118-124.

Bousse, T., T. Takimoto, K. G. Murti, and A. Portner. 1997. Elevated expression of the human parainfluenza virus type I F gene downregulates HN expression. Virol. **232**:44-52.

Bousse, T., T. Matrosovich, A. Portner, A. Kato, Y. Nagai, and T. Takimoto. 2002. The long noncoding region of the human parainfluenza virus type 1 F gene contributes to the read-through transcription at the M-F gene junction. J. Virol. **76**:8244-8251.

Bridgen, A. and R.M Elliott. 1996. Rescue of a segmented negative-strand RNA virus entirely from cloned complementary DNAs. PNAS. **93**:15400-15404.

Chanock, R.M., B.R. Murphy, and P.L. Collins. 2001.Parainfluenza Viruses. In "Fields Virology" (D.M. Knipe, and P.M. Howley, Eds.), 4th ed., pp.1341-1379. Lippincott Williams and Wilkins, Philadelphia.

Chen, W., P.A. Calvo, D. Malide, J. Gibbs, U. Schubert, I. Bacik, S. Basta, R. O'Neill, J. Schickli, P. Palese, P. Henklein, J.R. Bennink, and J.W.Yewdell. 2001. A novel influenza A virus mitochondrial protein that induces cell death. Nat. Med. **7**:1306-1312.

Clarke, D.K., M.S. Sidhu, J.E. Johnson and S.A. Udem. 2000. Rescue of mumps virus from cDNA. J. Virol. **74**:4831-4838.

Conzelmann, K-K. 1998. Nonsegmented negative-strand RNA viruses: genetics and manipulation of viral genomes. Annu. Rev. Genet. **32**:123-162.

Davuluri, R.V., Y. Suzuki, S. Sugano, and M.Q. Zhang. 2000. CART classification of human 5' UTR sequences. Genome Res. **10**:1807-1816.

Dawe, S. and R. Duncan. 2002. The S4 genome segment of baboon reovirus is biscistronic and encodes a novel fusion-associated small transmembrane protein. J. Virol. **76**:2131-2140.

Dimock, K., D.G. Storey, M-J. Côté and C.Y. Kang. 1987. Cloning, coding assignments and mapping of human parainfluenza virus 3 genes. In: "The Biology of Negative Strand Viruses" (Mahy and Kolakofsky, Eds.), pp. 213-220. Elsevier Science Publishers BV (Biomedical devision)

Drexler, I., K. Heller, B. Wahren, V. Erfle, and G. Sutter. 1998. Highly attenuated modified vaccinia virus Ankara replicates in baby hamster kidney cells, a potential host for virus propagation, but not in various human transformed and primary cells. J. Gen. Virol. **79**:347-352.

Durbin, A.P., S.L. Hall, J.W. Siew, S.S. Whitehead, P.L. Collins, and B.R. Murphy. 1997. Recovery of infectious human parainfluenza virus type 3 from cDNA. Virol. **235**:323-332.

Durbin, A. P., M. Skiadopoulos, J.M.McAuliffe, J.M. Riggs, S.R. Surman, P.L. Collins and B.R.Murphy. 2000. Human parainfluenza virus type 3 (PIV3) expressing the hemagglutinin protein of measles virus provides a potential method for immunization against measles virus and PIV3 in early infancy. J. Virol. **74**:6821-6831.

Ebata, S.N. 1996. Requirements for syncytium formation mediated by the fusion glycoprotein of human parainfluenza virus type 3. Thesis.

He, B., R.G. Paterson, C.D.Ward and R.A. Lamb. 1997. Recovery of infectious SV5 from cloned DNA and expression of a foreign gene. Virology **237**:249-260.

Henrickson, K.J. 2003. Parainfluenza viruses. Clin. Microbiol. Rev. **16**:242-264.

Hoffman, M.A. and A.K. Banerjee. 1997. An infectious clone of human parainfluenza virus type 3. J. Virol. **71**:4272-4277.

Itoh, M., H. Hotta and M. Homma. 1998. Increased induction of apoptosis by sendai virus mutant is associated with attenuation of mouse pathogenicity. J. Virol. **72**:2927-2934.

Jogalekar, P.P. 2000. Analysis of gene junction sequences of human parainfluenza virus type 3. Thesis.

Joshi, SB., R.E. Dutch and R.A. Lamb. 1998. A core trimer of the paramyxovirus fusion protein: Parallels to influenza virus hemagglutinin and HIV-1 gp41. Virology **248**:20-34.

Kim, K-S and C.K. Pallaghy. 1996. Purification of plasmid DNA (mini-prep) with high yields using diatomaceous earth, Molecular Biology Protocols, U.S. Department of Commerce Online Journal, http://micro.nwfsc.noaa.gov/protocols/dna-prep.html

Kolakofsky, D., T. Pelet, D. Garcin, S. Hausmann, J. Curran, and L. Roux. 1998. Paramyxovirus RNA synthesis and the requirement for hexamer genome length: the rule of six revisited. J. Virol. **72**:891-899.

Kowalski, P.E. and D.L. Mager. 1998. A human endogenous retrovirus suppresses translation of an associated fusion transcript, PLA2L. J. Virol. **72**:6164-6168.

Kozak, M. 1991. Structural features in eukaryotic mRNAs that modulate the initiation translation. J. Biol. Chem. **266**:19867-19870.

Kozak, M. 1997. Recognition of AUG and alternative initiator codons is augmented by G in position +4 but is not generally affected by the nucleotides in positions +5 and +6. EMBO J. **16**:2482-2492.

Kozak, M. 2002. Pushing the limits of the scanning mechanism for initiation of translation. Gene. **299**:1-34.

Krishnamurthy, S., Z. Huang, and S. K. Samal. 2000. Recovery of a virulent strain of newcastle disease virus from cloned cDNA: Expression of a foreign gene results in growth retardation and attenuation. Virol. **278**:168-182.

Lamb, R.A., and D. Kolakofsky. 2001. *Paramyxoviridae*: The viruses and their replication. In "Fields Virology" (D.M. Knipe, and P.M. Howley, Eds.),4th ed., pp.1305-1340. Lippincott Williams and Wilkins, Philadelphia.

Leduc, R., S.S. Molloy, B.A. Thorne, and G. Thomas.1992. Activation of human furin precursor processing endoprotease occurs by an intramolecular autoproteolytic cleavage. J. Biol. Chem. **287**:14304-14308.

Maresova, L., T.J. Paseika and C. Grose. 2001. Varicella-Zoster virus gB and gE coexpression but not gB or gE alone, leads to abundant fusion and syncytium formation equivalent to those from gH and gL coexpression. J. Virol. **75**:9483-9492.

McGinnes, L.W., K. Gravel and T.G. Morrison. 2002. Newcastle disease virus HN protein alters the conformation of the F protein at cell surfaces. J. Virol. **76**:12622-12633.

McKenna, N. 1999. Unpublished Data.

Meijer, H.A. and A.A.M.Thomas. 2002. Control of eukaryotic protein synthesis by upstream open reading frames in the 5'- untranslated region of an mRNA. Biochem. J. **367**:1-11.

Meyuhas, O. 2000. Synthesis of the translational apparatus is regulated at the translational level. Eur. J. Biochem. **267**:6321-6330.

Morris, D.R. and A.P. Geballe. 2000. Upstream open reading frames as regulators of mRNA translation. Mol. Cell. Biol. **20**:8635-8642.

Nakayama, K. 1997. Furin: a mammalian subtilisin/Kex2p-like endoprotease involved in processing of a wide variety of precursor proteins. Biochem. J. **327**:625-635.

Neumann, G., T. Watanabe, H. Ito, S. Watanabe, H. Goto, P. Gao, M. Hughes, D.R. Perez, R. Donis, E. Hoffmann, G. Hobom and Y. Kawaoka. 1999. Generation of influenza A viruses entirely from cloned cDNAs. PNAS. **96**:9345-9350.

Neumann, G., M.A. Whitt, and Y. Kawaoka. 2002. A decade after the generation of a negative-sense RNA virus from cloned cDNA- what have we learned? J. Gen. Virol. **83**:2635-2662.

Nussbaum, O., C.C. Broder, and E.A. Berger. 1994. Fusogenic mechanisms of enveloped-virus glycoproteins analyzed by a novel recombinant vaccinia virus-based assay quantitating cell fusion-dependent reporter gene activation. J. Virol. **68**:5411-5422.

Ortmann, D., M. Ohuchi, H. Angliker, E. Shaw, W. Garten, and H.D. Klenk. 1994. Proteolytic cleavage of wild type and mutants of the F protein of human parainfluenza virus type 3 by two subtilisin-like endoproteases, furin and Kex2. J. Virol. **68**:2772-2776.

Parks, G.D., K.R. Ward, and J.C. Rassa. 2001. Increased readthrough transcription across the simian virus 5 M-F gene junction leads to growth defects and a global inhibition of viral mRNA synthesis. J. Virol. **75**:2213-2223.

Peeters, B.H.P., O.S De Leeuw, G. Koch, and A.L.J. Gielkens. 1999. Rescue of Newcastle Disease Virus from cloned cDNA: evidence that cleavability of the fusion protein is a major determinant for virulence. J. Virol. **73**:5001-5009.

Porotto, M., M. Murrell, O. Greengard, and A. Moscona. 2003. Triggering of Human Parainfluenza Virus 3 fusion protein (F) by the hemagglutinin-Neuraminidase (HN) protein: an HN mutation diminishes the rate of F activation and fusion. J. Virol. **77**:3647-3654.

Radecke, F., P. Spielhofer, H. Schneider, K. Kaelin, M. Huber, C. Dotsch, G. Christiansen and M.A. Billeter. 1995. Rescue of measles viruses from cloned cDNA. EMBO J. **14**:5773-5784.

Rassa, J.C. and G.D. Parks. 1998. Molecular basis for naturally occurring elevated readthrough transcription across the M-F junction of the paramyxovirus SV5. Virol. **247**:274-86.

Reed, L.J and H. Muench. 1938. A simple method of estimating fifty per cent endpoints. Amer. J. Hyg. **27**:493-7.

Rouselle, J. Unpublished Data.

Sandberg, A.A., and A. Borgström. 2002. Early prediction of severity in acute pancreatitis. Is this possible. J.O. Pancreas (Online). **3**:116-125.

Schnell, M.J., T. Mebatsion, and K.K. Conzelmann. 1994. Infectious rabies viruses from cloned cDNA. EMBO J. **13**:314-322.

Seidah, N.G., and M. Chrétien. 1997. Eukaryotic protein processing: endoproteolysis of precursor proteins. Cur. Op. Biotechnol. 8:602-607.

Senanayake, S.D and D.A. Brian. 1999. Translation from the 5' untranslated region (UTR) of mRNA 1 is repressed, but that from the 5' UTR of mRNA 7 is stimulated in coronavirus-infected cells. J. Virol. **73**:8003-8009.

Sergel, T.A., L.W. McGinnes and T.G. Morrison. 2000. A single amino acid change in the newcastle disease virus fusion protein alters the requirement for HN protein in fusion. J. Virol. **74**:5101-5107.

Stone-Hulslander, J. and T.G. Morrison. 1997. Detection of an interaction between the HN and F proteins in Newcastle Disease virus-infected cells. J. Virol. **71**:6287-6295.

Storey, D.G. 1987. Structural characterization of human parainfluenza virus type 3 and cloning of viral specific genes. Thesis.

Tanaka, Y, B.R. Heminway, and M.S. Galinski. 1996. Downregulation of paramyxovirus hemagglutinin-neuraminidase glycoprotein surface expression by a mutant fusion protein containing a retention signal for the endoplasmic reticulum. J. Virol. **70**:5005-5015.

Tao, T., A.P. Durbin, S.S. Whitehead, F. Davoodi, P.L. Collins and B.R. Murphy. 1998. Recovery of a fully viable chimeric human parainfluenza virus (PIV) type 3 in which the hemagglutinin-neuraminidase and fusion glycoproteins have been replaced by those of PIV type 1. J. Virol. **72**:2955-2961.

Tong, S. and R.W. Compans. 1999. Alternative mechanisms of interaction between homotypic and heterotypic parainfluenza virus HN and F proteins. J. Gen. Virol. **80**:107-115.

Voet, D and J.G Voet. 1998. Biochimie. De Boeck Université, Paris. pp.398-400.

Volchkov, V.E., V.A.Volchkova, E. Muhlberger, L.V.Kolesnikova, M. Weik, O.Dolnik and H.D. Klenk. 2001. Recovery of infectious Ebola virus from complementary DNA: RNA editing of the GP gene and viral cytotoxicity. Science **291**:1965-1969.

Wong, T.C. and Hirano, A. 1987. Structure and function of bicistronic RNA encoding the phosphoprotein and the matrix protein of Measles virus. J. Virol. **61**:584-589.

Watanabe, M., A. Hirano, S. Stenglein, J. Nielson, G. Thomas, and T.C. Wong. 1995. Engineered serine protease inhibitor prevents furin-catalyzed activation of the fusion glycoprotein and production of infectious measles virus. J. Virol. **69**:3206-3210.

Watanabe, T., K. Murakami and K. Nakayama. 1993. Positional and additive effects of basic amino acids on processing of precursor proteins within the constitutive secretory pathway. FEBS **3**:215-218.

Wunschmann, S and J.T. Stapleton. 2000. Fluorescence based quantitative methods for detecting human immunodeficiency virus type 1-induced syncytia. J. Clin. Microbiol. **38**:3055-3060.

Young, J.K., R.P. Hicks, G.E. Wright, and T.G. Morrison. 1997. Analysis of a peptide inhibitor of paramyxovirus (NDV) fusion using biological assays, NMR and molecular modeling. Virology **238**:291-304.

APPENDIX

I had hypothesized during the course of my experimentation, that because syncytia are cells that are larger and more granular, one would be able to detect a population of fused cells by flow cytometry. This methodology has been used to detect HIV-1 induced syncytia in MT-2 (T cell line) cell culture (Wunschmann and Stapleton, 2000). To explore this possibility, I first carried out a number of simple experiments, as proof of principle. The first experiment was to trypsinize a monolayer of fused HeLaT4 cells to determine whether or not the fused cells were too fragile to be used in flow cytometry. The cells, when trypsinized all appeared to remain intact, the detached syncytia could be seen through the microscope. The next experiment that I pursued was to fix the cells in paraformaldehyde and perform flow cytometry on fused and unfused HeLaT4 cells. Unfortunately, it was determined that HeLaT4 cells, already quite large, when fused were not detectable by the Coulter EPICS XL-MCL, Beckmann Coulter. Another experiment was carried out, using ethanol to fix the cells instead of paraformaldehyde. The hypothesis for this experiment was that the ethanol would dehydrate the cells and possibly allow the detection of the larger syncytia. This experiment yielded results similar to the one with the paraformaldehyde fixed cells. I also stained the cells with propidium iodide, a nucleic acid stain, in an attempt to distinguish cells with one nucleus from those with multiple nuclei. This was unsuccessful. The final experiment was the same as this last experiment, except that the instrument was changed, a MoFLOW by Cytomation was used. However, this new instrument could not detect the multinucleated cells either. This method is promising if a smaller cell line, resistant to vTF7-3 cytopathic

effect, can be found and in which HPIV3 F and HN induced fusion can occur. Smaller cells will give rise to syncytia that are within the detection limits of the instrument.